Available online at www.sciencedirect.com
SCIENCE DIRECT®
Ore Geology Reviews 28 (2006) 32–56
ORE GEOLOGY REVIEWS
www.elsevier.com/locate/oregeorev

Geochemical and mineralogical distribution of germanium in the Khusib Springs Cu–Zn–Pb–Ag sulfide deposit, Otavi Mountain Land, Namibia

Frank Melcher *, Thomas Oberthür, Dieter Rammlmair

Federal Institute for Geosciences and Natural Resources (BGR), Stilleweg 2, 30655 Hannover, Germany

Received 1 April 2003; accepted 12 April 2005
Available online 25 October 2005

Abstract

The Khusib Springs deposit in the Otavi Mountain Land, Namibia, is a small though high-grade carbonate-hosted Cu–Zn–Pb–Ag–(As–Sb–Ge) deposit of the "Tsumeb-type" containing approximately 300,000 t of ore grading 10% Cu, 1.8% Pb and 584 ppm Ag. A lens-shaped sulfide orebody, up to 10 m thick and elongated parallel to bedding, replaces limestone, locally brecciated, of the lower Tsumeb Subgroup (Damara Supergroup) in the northern limb of a large NE-trending synclinal structure. A prominent zone of dolomite alteration surrounds the orebody. In a drill core through the orebody, the uppermost 2 m are enriched in Zn (up to 5%) and Ag (up to 3350 ppm), but lower in Ge (<30 ppm) than the central and lower parts of the orebody, which are in turn enriched in Ge (up to 200 ppm) and Pb (up to 7%). Massive ore consists of a texturally complex mineral assemblage dominated by Zn-rich tennantite, enargite, galena and pyrite. Fe-poor sphalerite is abundant only in the uppermost part of the orebody and in the footwall where it forms a prominent zone of disseminated sphalerite ± chalcopyrite ± galena ± pyrite. The upper zone of the massive ore is further characterized by a general lack of enargite, and the occurrence of a variety of late-stage phases including tetrahedrite, Ag-bearing tennantite, pearceite–polybasite and native silver. The central and lower parts of the orebody are composed of tennantite–enargite–galena ore with variable proportions of pyrite, but lacking sphalerite. Most Ge is hosted in Ge-bearing colusite [$Cu_{26}V_2(As,Ge)_6S_{32}$] forming small (usually <50 μm in size) grains along the margins of ore layers and veinlets. With the notable exception of enargite, the major sulfides contain only trace amounts of Ge (<100 ppm). Trace element analyses reveal a wide range of Ge concentrations in enargite, averaging to 500 ppm. Frequently, colusite is associated with deformed trails of phengitic, F-rich muscovite, rutile, apatite, tourmaline, dolomite and pyrite. Such trails are interpreted as former stylolites in the carbonate host rock, which has been replaced by sulfide ore. Colusite carries on average 4.0 wt.% Ge, up to 4.7 wt.% W and up to 4.4 wt.% Sn, and is occasionally accompanied by small amounts of Mo–W sulfides. Additional minerals identified in the ore include W-bearing germanite, Ge-bearing stannoidite, chalcopyrite, bornite, stromeyerite, minerals of the chalcocite-group, and covellite.

Geochemical and mineralogical features of sulfide ores from Khusib Springs resemble some sulfide ores of the pipe-shaped polymetallic Ge-rich Tsumeb deposit. Similar to the latter, ore formation probably occurred during D_2 deformation and metamorphism and involved highly saline, hot brines (up to 370 °C [Chetty, D., Frimmel, H.E., 2000. The role of evaporites in the genesis of base metal sulfide mineralization in the Northern Platform of the Pan-African Damara Belt, Namibia: geochemical and fluid inclusion evidence from carbonate wall rock alteration. Mineralium Deposita 35, 364–376]) carrying sulfur derived from evaporite sequences. A polyphase mineralization involving three successive stages is proposed: early sphalerite–pyrite–(chalcopyrite–bornite) mineralization is replaced by tennantite, enargite, galena and Ge-bearing colusite. A late stage mineralization

* Corresponding author. Fax: +49 511 643 3664.
E-mail address: F.Melcher@bgr.de (F. Melcher).

doi:10.1016/j.oregeorev.2005.04.006

overprints parts of the orebody at lower temperatures leading to precipitation of 'schalenblende' (Cu- and Ag-rich), digenite, tetrahedrite and pearceite–polybasite. The occurrence of small, but high-grade Ge-rich Cu–Zn–Pb–Ag deposits in the lower Tsumeb Subgroup has important consequences on the mineral potential of the area, because prospecting for Cu-rich ores has been traditionally performed in the uppermost Tsumeb Subgroup only, in relation to paleokarst structures.

Keywords: Germanium mineralization; Otavi Mountainland; Namibia; Colusite; Tennantite; Tsumeb-type deposit

1. Introduction

Germanium (Ge) is an important high-technology electronic metal, finding increasing use in fiber and infrared optics, and as polymerization catalysts (George, 2003). World refined Ge production (50 tons in 2004; George, 2005) can no longer meet the demand of the world market; the difference is balanced by recycling (35%) and releases from stockpiles. As estimated global resources are a few thousand tons of recoverable Ge only (Höll et al., this volume), there is a strong demand for exploration and for innovative extraction techniques.

Carbonate-hosted base metal sulfide deposits are an important source of Ge. The richest, though rare, deposits are epigenetic, discordant polymetallic deposits of the 'Kipushi-' or 'Tsumeb'-type, which are frequently associated with karst features (cf. Höll et al., this volume). Examples include Kipushi/D.R. Congo, Kabwe/Zambia, Apex/USA and Tsumeb/Namibia. Such depos-

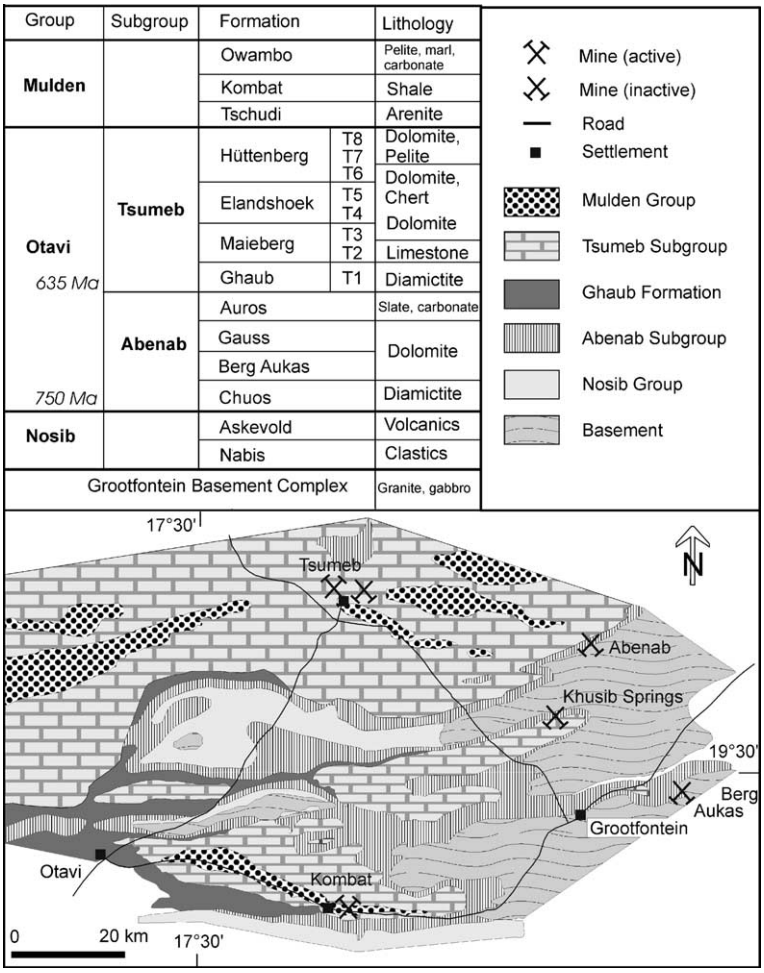

Fig. 1. Stratigraphy and simplified geological map of the Otavi Mountain Land (OML) in Namibia (modified after Chetty and Frimmel, 2000). Approximate ages for deposition of the Chuos and Ghaub Formations after Fölling and Frimmel (2002) and Hoffman et al. (2004).

its are characterized by the occurrence of Cu–thiogermanate minerals, e.g., germanite, reniérite, briartite and germanocolusite. Carbonate-hosted, strata-bound, low-temperature Zn–Pb sulfide deposits, a highly diverse group of deposits commonly referred to as the "Mississippi Valley-type" (MVT, cf. Leach et al., 2001), are much more common than Kipushi- or Tsumeb-type deposits. Although Ge grades usually are lower, they are the major world suppliers due to their abundance. Germanium, which substitutes for Zn in the sphalerite and wurtzite structures, is recovered as a by-product from zinc ores (Höll et al., this volume).

The world-famous Tsumeb deposit, situated in the Otavi Mountain Land (OML), Namibia, was one of the largest deposits of the Tsumeb-type until its closure in 1996. Tsumeb is hosted by Neoproterozoic dolomites of the Otavi Group within the Damara Supergroup (Lombaard et al., 1986). Between 1905 and 1996 the mine produced about 30 Mt of ore grading 10% Pb, 4.3% Cu, and 3.5% Zn. Significant quantities of Ge, As, Sb, Ag, Cd, and Au have been extracted. Ore from Tsumeb contained on average 50 ppm Ge (Lombaard et al., 1986).

More than 600 occurrences of Cu–Pb–Zn–V mineralization are known in the Otavi Mountain Land (Cairncross, 1997). Among them, the high-grade Khusib Springs deposit was discovered early in the 1990s through mapping and drilling, and went into production in 1995. Before liquidation of the Tsumeb Corporation Limited (TCL) in 1997, 107,000 t of ore have been mined, from which 21,473 t Cu concentrates grading 26% to 28% Cu have been produced (Coakley, 1997). Between October 2000 and August 2002, another 45,000 t ore has been mined by the new owner, Ongopolo Mining and Processing Limited. In 2000, proven reserves were 119,000 t grading 10% Cu, 1.82% Pb and 584 ppm Ag (Coakley, 2000). Meanwhile, production has stopped (Ongopolo, personal communication).

Based on geochemical and fluid inclusion data obtained on different carbonate generations, the Khusib Springs deposit is believed to be of the Cu-rich 'Tsumeb-type' (Verran, 1996; Chetty et al., 1997; Chetty and Frimmel, 2000), which, among other features, is distinguished from the 'Berg Aukas-type' deposits (Cu-poor Pb–Zn deposits with similarities to MVT deposits) of the OML by having significantly higher trace element concentrations (Frimmel et al., 1996). In order to evaluate the potential of Tsumeb-type deposits for metals with a short lifetime of reserves (defined here as those high-technology metals having reserves of less than 25 years at constant demand), the German Federal Institute for Geosciences and Natural Resources (BGR) is conducting a geological research project in the Otavi Mountain Land. In this contribution we present a detailed report on the mineralogy and geochemistry of the sulfide ores from Khusib Springs (Fig. 1), with the main focus on the concentration, mineralogical siting and metallogenic position of Ge in the ores. The relation to the Ge-rich Tsumeb deposit is discussed.

2. Geological background

The Neoproterozoic Damara Supergroup in the Otavi Mountain Land (Fig. 1) is subdivided, from bottom to top, into the Nosib (clastic sediments and volcanics), Otavi (mainly carbonates) and Mulden Groups (clastic molasse-type sediments). The Otavi Group, deposited between approximately 750 and 545 Ma and hosting most orebodies in the OML, is subdivided into the Abenab and Tsumeb Subgroups. Sedimentation in both subgroups started with glacial diamictites (the Chuos and Ghaub Formations, respectively), followed by carbonate sedimentation on a shallow shelf. Carbonates of the Abenab Subgroup mainly host Berg Aukas-type Zn–Pb mineralization with appreciable supergene enrichment of vanadium (e.g., the former Abenab West and Berg Aukas mines; Fig. 1). The Tsumeb Subgroup mainly contains Cu-rich Tsumeb-type deposits, although Berg Aukas-type mineralization is known from several locations. Eight informal lithozones (T1 to T8; Hedberg, 1979) are distinguished within the Tsumeb Subgroup (Fig. 1). The Khusib Springs deposit is located in laminated limestones of the Maieberg Formation (T2 lithozone) of the Tsumeb Subgroup, close to the contact with laminated dolomicrite of lithozone T3 (Fig. 1). Sedimentological and carbon isotope studies indicate that the Maieberg Formation was deposited in relatively deeper water than the remaining Tsumeb Subgroup during a collision event in the Kaoko Belt further to the west (Hedberg, 1979; Kaufman et al., 1991; Frimmel et al., 1996), and in cold water following a glacial episode which is preserved in the underlying Ghaub Formation (T1). The age of the glaciation is a contentious issue; while Hoffman et al. (1998) argue for a Sturtian age (760 to 700 Ma) of the whole Otavi Group, other authors (Kennedy et al., 1998; Fölling and Frimmel, 2002) favor a syn-Marinoan/Varangian age (635.5 ± 1.2 Ma; Hoffman et al., 2004) of the Ghaub Formation.

Continent–continent collision between the Congo and Kalahari Cratons resulted in deformation and regional metamorphism (D_2) in the Damara Belt approximately 545 Ma ago (Frimmel and Frank, 1998). In the

OML, D_2 deformation induced E–W-trending open to isoclinal F_2 folds and north-vergent thrusts with the intensity of deformation and metamorphism decreasing towards the north. Subsequent folding and thrusting onto the Kalahari Craton is documented by NE-trending open, upright cross-warps (D_3).

3. Sample description and mineralogy

The Khusib Springs mine is situated on the northern limb of a large NE-trending, westerly plunging synformal structure (the Harasib–Olifantsfontein syncline, Fig. 1). The laminated limestones of the Maieberg Formation (T2-zone) dip approximately 25° to the south. Drilling in stratigraphically lower parts of the T2-zone north of Khusib Springs identified low-grade sulfide mineralization (pyrite, pyrrhotite, chalcopyrite, sphalerite) in laminated slaty limestone. In surface outcrop, a variety of breccias were distinguished at Khusib Springs (Verran, 1996), including synsedimentary rip-up breccia and subordinate dolospar-supported polymictic breccia. Most conspicuous is a matrix (dolomite)-supported polymictic breccia along the T2/T3 contact. Open kink and box folds associated with local crackle breccias formed during E–W compression (D_3). The most notable structural feature in the mine area is an offset of the T2 and T3 contacts by about 260 m (Verran, 1996).

The orebody forms a lens-like structure oriented parallel to bedding, dipping 40° to the south (Fig. 2). In surface outcrop mineralization is indicated by weak impregnation of azurite, malachite and some chalcocite and tennantite. The orebody is a semi-continuous lens down to 300 m below surface, separated into an upper and a lower body by a zone at 110 m depth where the orebody almost pinches out. The upper orebody reaches approximately 150 m in its longest dimension and a thickness of more than 10 m. A strata-bound zone of dolomite alteration surrounds the ore. Considerable drilling was undertaken to identify a possible downdip extension of the orebody. Subeconomic, disseminated mineralization of tennantite and pyrite, with minor sphalerite, galena and chalcopyrite was found in steeply dipping brecciated limestone, e.g., in a vertical drill hole at a depth of 360 to 380 m below surface (KH66, 180 m south of KH26).

Samples for this study were taken from stopes, dumps and drill cores. In core KH26, drilled at an angle of 50° to the North and cutting almost perpendicular through 127.7 m of carbonate rock, the sulfide orebody was intersected between 81.5 and 91.8 m (Fig. 2). Low-grade disseminated mineralization containing galena, tennantite, covellite, digenite and pyrite is occasionally present in the hanging-wall between 25.9 and 80.3 m, and in the footwall at 92.7 m (Fig. 3). The carbonate host rocks are fine-grained, equigranular, partly laminated dolomitized limestones containing small amounts of quartz, white mica, potassium feldspar, apatite, rutile and zircon. Vein stockworks of coarse sparitic dolomite and calcite occur in all levels of the core, but at different vein densities (Fig. 4 A, B). Such veins may also contain fibrous quartz. Stylolites

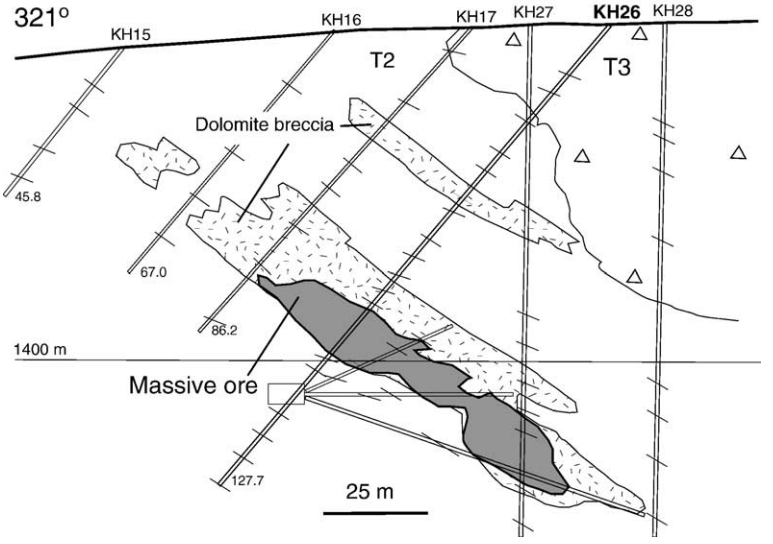

Fig. 2. Cross-section of the Khusib Springs deposit showing, among others, the location of drill hole KH26 (Ongopolo Mining and Processing Ltd., unpublished data).

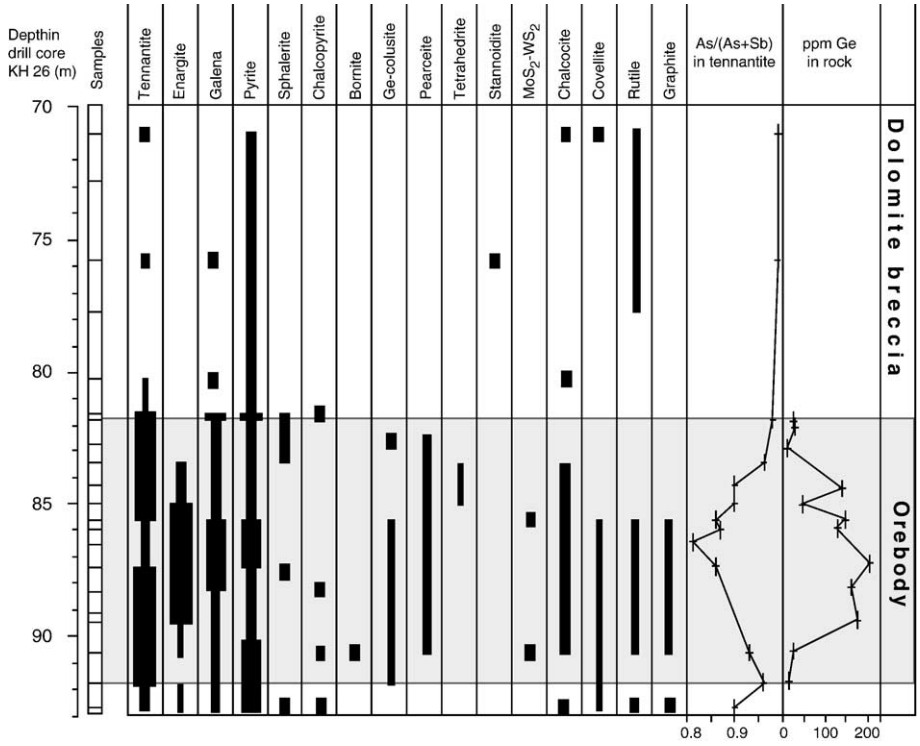

Fig. 3. Schematic section through the lower part of drill core KH26 (70–93 m) illustrating variations in the contents of opaque minerals. Line thickness corresponds to relative abundances. Average molar As/(As+Sb) concentrations in fahlore determined by microprobe, and Ge concentrations in whole rock sample splits are displayed (see also Fig. 6).

are abundant and carry organic matter (semigraphite) besides small amounts of rutile and pyrite. Euhedral apatite grains up to 50 μm in size are abundant close to the massive sulfide zone. Large segments of the drill core are brecciated (i.e., between 33 to 50 m, and below 70 m), with clasts of both micritic and sparitic limestone cemented by coarse white dolosparite. Calcitic limestone is predominant above 24 m, between 40 to 47 m, 51 to 72 m, and below 93 m (Fig. 2). These rocks are not as strongly affected by sparitic veining and brecciation as the dolomitic limestones, and carry remarkably lower concentrations of Cu, Pb and Zn. Chetty and Frimmel (2000), Gross and Vollbrecht (2003), and Melcher et al. (2003) distinguished a number of carbonate generations in the Khusib Springs deposit. The host rock is usually either dolomicrite (dolomite I after Chetty and Frimmel, 2000) or micritic limestone (limestone I), which is in places dark and rich in hydrocarbons. Dolomite II occurs as sparry veins hosting sulfide mineralization, and as coarsely recrystallized dolomite I. Sparry dolomite (dolomite III) fills veins or forms a breccia matrix, hosting oxidation products such as malachite and azurite, but no sulfides. Late-stage, post-mineralization, crosscutting veins are filled by calcite I. Cathodoluminescence investigations show bright red luminescence in dolomite II and III and yellow colors in calcite I.

In drill core KH26, the sulfide orebody is about 10 m thick and texturally complex. In decreasing order of abundance, the following sulfides were identified (Table 1, Fig. 3): tennantite (on average >40 vol.%), enargite (~20 vol.%), pyrite (~20 vol.%), galena (~10 vol.%), and subordinate to rare sphalerite, chalcocite-group minerals, covellite, Ge-bearing colusite, pearceite–polybasite, tetrahedrite, chalcopyrite, bornite, stromeyerite, stannoidite, and W–Mo sulfides. In addition, rutile and (semi)graphite are locally abundant. Massive sulfide ore replaces laminated carbonate rock as well as carbonate breccia. The mineralization occurs either in concordant or discordant massive veins, as mottled, more disseminated ore, or as breccia ore (Fig. 4C). Starting from discordant veinlets, narrow ore stringers develop parallel to the sedimentary lamination. Mineralogical and chemical zoning is developed in many sulfide layers and veins. In their central parts, they consist of coarse-grained tennantite and enargite with pore fillings of white dolosparite or calcite (Fig. 4A, B), whereas the rims are characterized by smaller grain size, lamination, and frequent inclusions of silicates (muscovite, tourmaline, K-feldspar), rutile, and

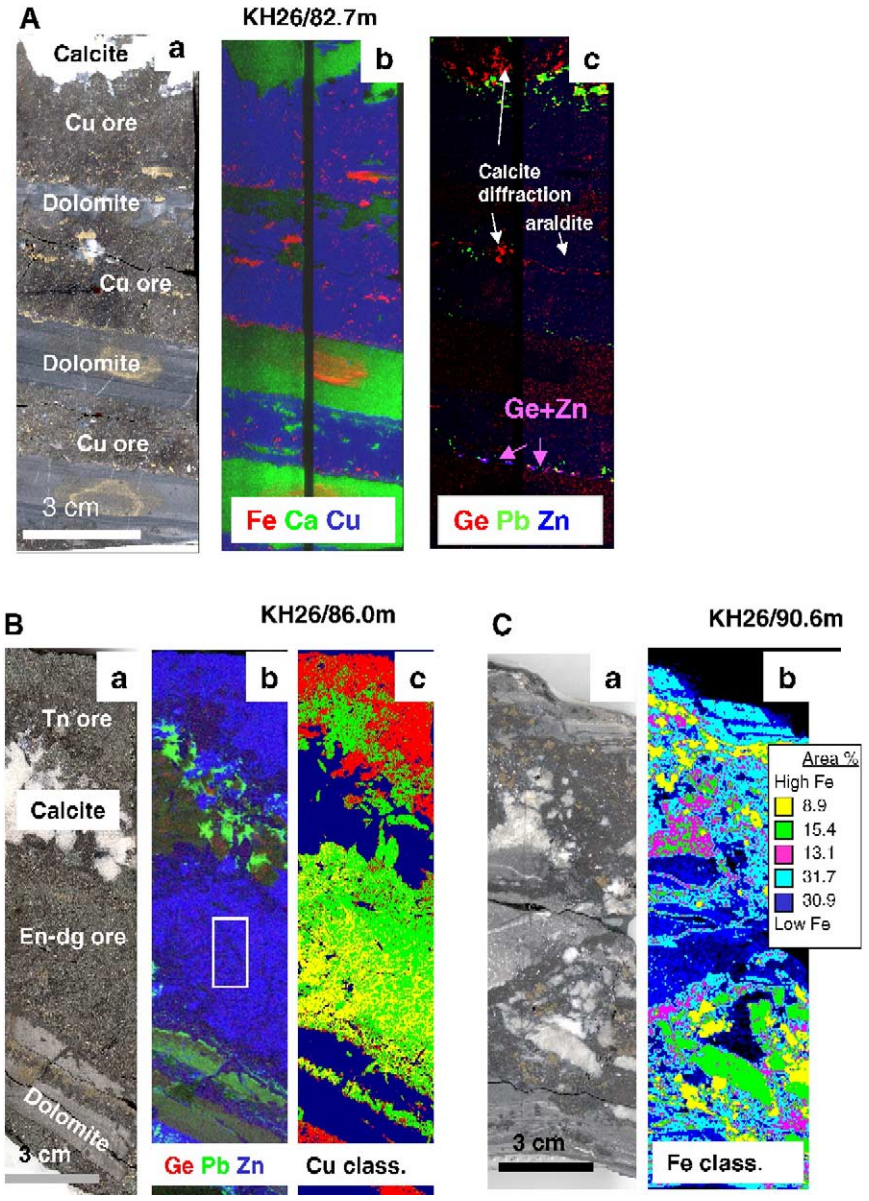

Fig. 4. Optical scans and element scans of drill core slabs (KH26) using μ-XRF (Geoscanner). (A) Cu ore (tennantite+pyrite+sphalerite) from 82.7 m; (a) optical scan; (b) overlay of Fe (red), Ca (green) and Cu concentrations (blue); (c) overlay of Ge (red), Pb (green) and Zn concentrations (blue). Violet colors correspond to areas where both Zn and Ge are present. (B) Tennantite (Tn) ore and enargite–digenite (En–dg) ore from 86.0 m; (a) optical scan; (b) overlay of Ge (red), Pb (green) and Zn (blue); (c) Cu concentration map, classified into 4 colors: yellow (very high), intermediate (green), low (red), none (blue). Elevated Ge concentrations along the deformed stylolite, only visible at higher magnification, are shown in the white box. (C) Breccia ore from 90.6 m; (a) optical scan; (b) Fe concentration map, classified into 5 groups, from yellow (very high) to dark blue (low Fe concentrations).

abundant pyrite. Pyrite is present as large, euhedral crystals, or almost monomineralic aggregates in massive ore, or as euhedral to subhedral inclusions throughout the ore. Tennantite, and tennantite–enargite intergrowths form the bulk of the ore, carrying inclusions of galena and pyrite, and developing mosaic textures in places. Enargite is absent in the upper parts of drill core KH26 (Fig. 3). Below a depth of 83 m, it is commonly present as anhedral inclusions in tennantite, approximately 100 μm in size; in some samples, however, enargite is the major sulfide mineral and carries inclusions of tennantite, pyrite and galena. Chalcopyrite is rare, occurring as inclusions in pyrite, tennantite and sphalerite only. In contrast to the Tsumeb

Table 1
Ore mineral assemblage in sulfide ore of the Khusib Springs deposit

Mineral	Formula	Abundance	Composition	Early	Main	Late
Tennantite	$(Cu,Zn,Fe)_{12}As_4S_{13}$	••••	XAs 0.81-0.99 Ag 0.3, Ge <0.01	—	—	
Tetrahedrite	$(Cu,Zn,Fe)_{12}Sb_4S_{13}$	•	XAs <0.3, Ag <0.8			—
Ag-tennantite	$(Cu,Zn,Fe,Ag)_{12}As_4S_{13}$	•	Ag 2-15			—
Enargite	Cu_3AsS_4	•••	Ag 0.21, Ge <0.01	—	—	
Galena	PbS	•••	Se 0.18		—	—
Pyrite	FeS_2	•••	Cu 0.7; Co,Ni 0.05	—	—	
Sphalerite(I)	ZnS	••	Fe 1, Cd 0.2	—		
Sphalerite(II)		••	Fe <0.1, Cd 0.2	—		
Sphalerite (III)		••	Cu 1-3, Ag <1.8			—
Chalcopyrite	$CuFeS_2$	•		—		
Bornite	Cu_5FeS_4	∘		—		
Chalcocite-group	$Cu_{1.7-1.9}S$	••	Ag <1.3			—
Covellite	CuS	•	Ag 0.2-2.3			—
Pearceite–polybasite	$(Ag,Cu)_{16}As_2S_{11}$	••	Ag 40-58, Sb <2.5		—	—
Stromeyerite	CuAgS	∘		—		
Stannoidite	$Cu_8(Fe,Zn)_3Sn_2S_{12}$	∘	Ge 0.6	—		
Ge–Colusite	$Cu_{26}V_2(As,Ge)_6S_{32}$	••	Ge 4.0, W 0.9		—	
Germanite	$Cu_{26}Fe_4Ge_4S_{32}$	∘	W <5.4	—		
Molybdenite–Tungstenite	$(W,Mo)S_2$	•		—	—	—
Native Silver	Ag	∘				—
Rutile	TiO_2	•••		—		
Graphite	C	••		—		

Notes: •••• very frequent, ••• frequent, •• moderately abundant, • rare, ∘ very rare.
XAs = molar As/(As+Sb); element concentrations as averages, ranges (–) or maxima (<) in wt.%.
The relative paragenetic position is indicated by Early, Main and Late stages, repectively.

and Kombat (Fig. 1) mines, bornite is very rare at Khusib, having been detected only as part of minute polyphase inclusions with chalcopyrite and galena in pyrite. Sphalerite distribution is antithetic to enargite, and restricted to the upper (marginal) part of the orebody and to the footwall (Fig. 3). Enargite and to a lesser extent tennantite are replaced by digenite, and rarely by covellite.

Ge-bearing colusite is the only significant carrier of Ge as a major element in the ore and is moderately abundant downhole from 82.7 m (Figs. 3, 5a, b). Colusite forms anhedral to subhedral grains, 10 to 100 μm in size, along the rims of sulfide ore laminae, and is hosted by tennantite, enargite, pyrite, dolomite and muscovite. Small amounts of Mo–W sulfides are associated with colusite in a few samples. Sn-rich sulfides (stannoidite) occur as inclusions in tennantite in a sample of disseminated ore 5 m above the main orebody (Figs. 3 and 5c). Silver-rich sulfosalts (pearceite–polybasite), stromeyerite [CuAgS], Sb-rich fahlore (tetrahedrite) and argentian tennantite occur in small amounts and are texturally attributed to a late stage of ore formation (Fig. 5d–f). Native silver is present as platelets up to 0.5 cm long along the rims of sulfide layers or in vugs. Compared to the Tsumeb mine, minerals characteristic of the oxidation zone are rare at Khusib. Small amounts of malachite, azurite, duftite, cerussite, wulfenite, Ca–Fe–Zn carbonate and native Cu were identified.

4. Geochemistry of the ore

Major and trace elements were analyzed in sample splits using X-ray fluorescence analysis after alkali borate fusion (XRF at BGR), instrumental neutron activation analysis (INAA) and inductively coupled plasma mass spectrometry following total digestion (ICP-MS; INAA and ICP-MS by Activation Laboratories, Canada). Sulfur and Pb isotope ratios were also measured by ActLabs. At BGR, Philips PW-2400 (Rh tube) and PW-1480 (Cr tube) instruments were used. Partial analyses of sulfide-rich samples are presented in Table 2. Significant differences are observed for concentrations of Ge: values measured by ICP-MS (ActLabs) are lower than XRF (BGR) values. This is attributed to partial volatilization of Ge during total digestion. The concentrations of Ge obtained by XRF were tested against the GXR-3 standard (110 ppm Ge); lower limits of detection are 8 to 10 ppm in sulfide ore. Both data sets for Ge correlate with a coefficient of 0.8; therefore, the total digestion data are also reported in Table 2. Analyses from additional samples taken underground and on mine dumps, and

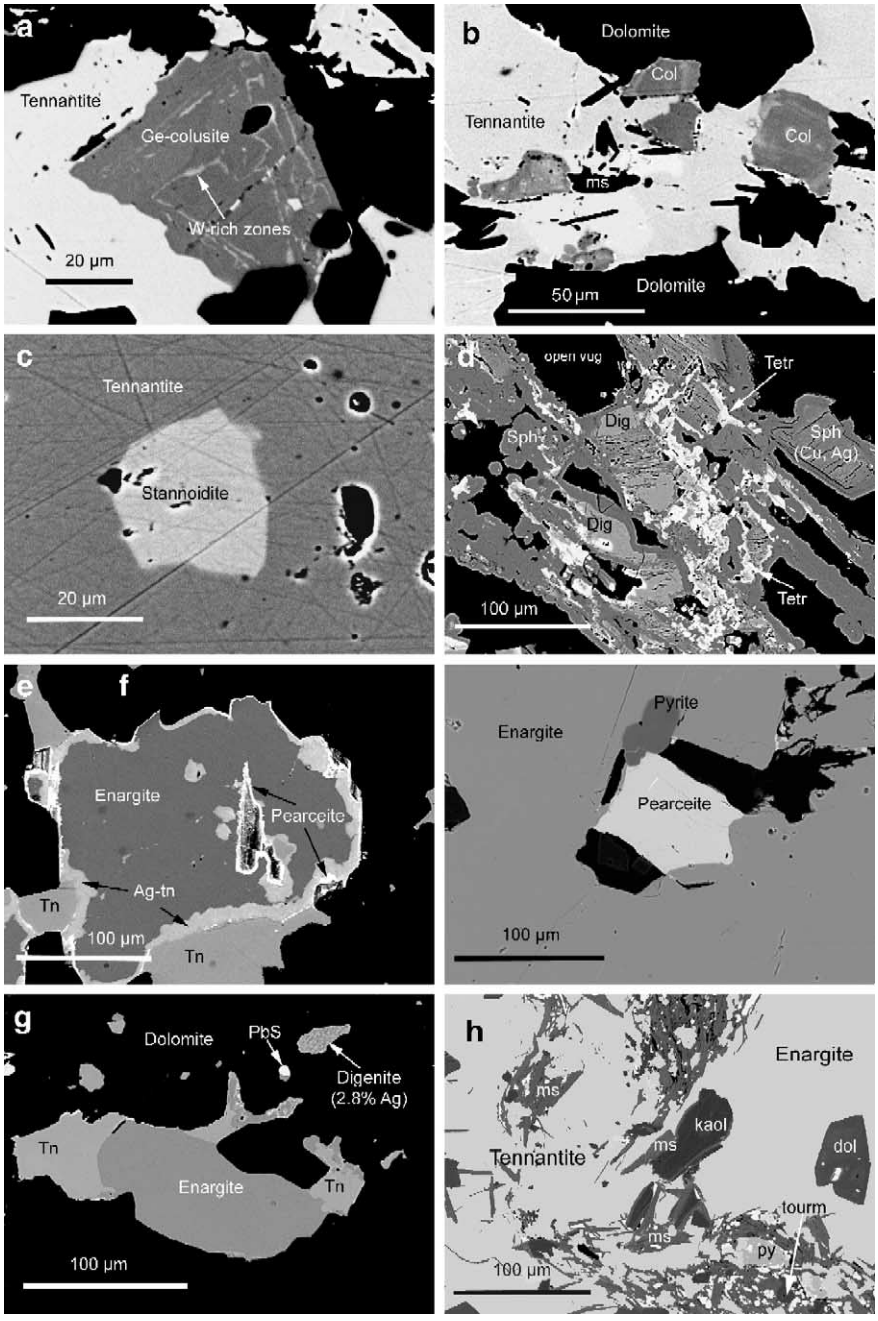

Fig. 5. Back-scatter electron images: (a) Ge-bearing colusite with zones rich in W, intergrown with tennantite and pyrite (black). Sample AS6459, KH26/86.4 m, (b) Ge-bearing colusite (Col) at tennantite–dolomite contact in sphalerite-bearing ore. Colusite carries variable W and Sn contents (brighter colors). Ms = muscovite. Sample AS6454a, KH26/82.7 m, (c) Ge-bearing stannoidite included in tennantite having 1 wt.% Ag; disseminated mineralization in the hanging-wall of the orebody, KH26/75.8 m; see Table 4, (d) Late-stage assemblage of digenite (Dig), sphalerite III (Sph) with elevated Cu and Ag, and tetrahedrite (Tetr) along open vugs of tennantite–enargite ore. Sample AS6593 (KH26/83.4 m), (e) Enargite (0.2 to 0.3 wt.% Ag) with reaction rim of Ag–bearing tennantite (5 to 6 wt.% Ag) and some pearceite against tennantite (Tn). Sample AS6461 (KH26/90.6 m), (f) Pearceite–polybasite and pyrite included in enargite. Sample AS6457, KH26/86.0 m, (g) Ge-bearing tennantite (Tn) and enargite in dolomite vein in the footwall of the orebody (KH26/92.7 m). See analyses in Table 4, sample KH92.7, (h) Deformed stylolite in massive tennantite–enargite ore, with phengitic, Fe-free and F-rich muscovite (ms), dolomite (dol), kaolinite (kaol), dravitic tourmaline (tourm) and pyrite (py). Sample AS6595, KH26/85.6 m.

Table 2
Whole-rock chemical analyses of sulfide ore from Khusib Springs

Sample	KH26	KH26	KH26	KH26	KH26	KH26	KH26	KH26	KH26	KH26	KH26	KH26	KH26	KH26	KS-03	KS-08	KS-10	KS-12	KS-15
depth	81.6	81.8	82.7	84.3	85.0	85.6	86.0	86.4	87.4	88.3	89.0	89.2	89.4	90.6	dump	2 Level	3 Level	5 Level	5L footwall
(wt.%)																			
S	9.80	14.41	20.34	19.87	15.34	20.25	22.23	20.27	18.21	16.16	21.56	21.57	21.16	9.96	18.37	15.25	7.31	6.67	10.78
SiO_2[a]	5.48	3.45	0.12	0.95	3.33	5.44	0.56		5.13	<0.10				3.02					
Al_2O_3	1.21	0.98	0.09	0.49	1.00	1.94	0.27	0.57	1.43	0.32	0.13	0.59	1.15	1.06	1.58	0.25	0.06	0.11	1.49
Fe_2O_3	1.12	2.60	2.44	3.19	3.17	3.37	3.62	4.26	4.63	0.80	4.35	5.73	4.66	2.76		1.49	0.07	0.59	0.90
MgO	12.09	9.69	2.86	2.55	9.70	7.32	0.31	5.52	5.15	6.66	2.45	4.29	4.56	11.79	1.66	5.46	9.59	9.54	3.22
CaO	15.37	13.65	3.65	3.06	12.43	8.42	0.20	3.96	7.39	10.50	2.39	3.97	4.04	14.56	2.03	7.35	13.70	13.44	18.86
Na_2O	0.07	0.04	0.05	0.05	0.04	0.04	0.04	0.07	0.04	0.11	0.15	0.07	0.07	0.03	0.03	0.04	0.03	0.03	0.01
K_2O	0.55	0.42	0.03	0.08	0.25	0.79	0.12	0.27	0.39	0.10	0.02	0.25	0.60	0.18	0.86	0.10	0.03	0.03	0.70
(in ppm)																			
Ag	1390	2060	3150	3350	770	590	2140	1120	434	2380	2080	769	835	581	1350	611	121	800	22
As	70600	96300	147000	138000	80000	87100	135000	116000	92100	92800	139000	122000	121000	64500	96300	106000	177	78000	426
Ba	68[a]	72[a]	35[a]	69[a]	53[a]	73[a]	40[a]	38	51[a]	52[a]	9	36	5	57[a]	11	10	4	7	23
Bi	0.26	0.26	0.77	0.35	1.29	0.64	1.15	1.74	0.30	3.03	0.32	0.53	0.39	1.16	2.59	0.22	0.73	0.08	
Cd	128	203	333	116	85	46	181	142	36	60	141	77	71	86	145	58.5	12.5	163	779
Co	19	42	56	46	43	36	76	34	26	18	86	68	53	13	30.4	28.8	0.3	2.8	4.9
Cu	153600	235000	354300	327300	216200	297900	412900	357600	256500	268200	416300	366030	345050	152800	267200	321100	559	184200	1920
Hg	18	20	45	21	22	11	51	6	11	10	30	19	21	28	15	12	14	11	21
Ga								6			13	7	7		20.8	5.8	0.1	17.3	35.2
Ge	9.3	6.6	2.5	55.9	21.8	108.9	24.0	39.7	83.8	33.4	34.4	18.4	42.2	7.0	60.1	55.4	1.1	5.4	
Ge[a]	26	28	13	140	49	148	128		203	161				26					
Mn	2002	1654	1998	1049	1211	972	1192	1350	1032	1071	1182	982	895	1697	665	1147	1957	2204	573
Mo	<2	<2	<2	<2	<2	<2	<2	<2	<2	64	<2	<2	<2	91	5	<1	<1	<1	<1
Ni	<3	<3	<3	<3	<3	<3	<3	<3	<3	<3	15	29	23	<3	5	9	2	4	5
Pb	1635	6573	8631	10940	10110	10030	16470	50590	10510	33440	17020	26490	22380	30780	10780	20500	514300	1260	145
Sb	4680	5720	13200	10600	9110	8530	17800	17200	6040	2920	9120	7160	7240	12700	13400	6390	174	1030	18.1
Se	23	38	78	86	68	63	131	208	75	145	46	69	60	109	95	73	230	21	14
Sn	5[a]	<2[a]	17[a]	29[a]	14[a]	26[a]	103[a]		20[a]	15[a]				19[a]	<1	<1	<1	6	2
Sr	90	74	29	17	70	48	8	24	43	43	16	23	21	85	16	39	75	84	113
Te	1.13	1.83	0.86	0.90	0.29	0.20	0.11		0.14	0.47	0.11	0.15	0.21	0.35	0.4	0.2	1.3	2.2	0.1
Tl	0.14	0.14	0.16	0.44	0.35	0.64	0.43	0.26	0.26	0.24	0.28	0.24	0.31	0.27	0.34	0.52	0.28	0.20	0.14
Th	<0.2	<0.2	8.80	<0.2	<0.2	<0.2	<0.2	0.14	<0.2	<0.2	<0.5	0.59	1.00	<0.2	1.3	0.2	0.1	0.1	0.6
U	<6	<7	<20	<20	<10	<10	<20	0.78	<20	<5	<0.5	0.62	1.27	<20	1.7	0.3	0.1	<0.1	0.7
V	8	5	<2	<2	<2	20	<2	10	3	13	<2	5	13	10	9	<1	2	8	13
W	69[a]	40[a]	30[a]	19[a]	12[a]	<5[a]	159[a]	<20	9[a]	<5[a]	<20	<20	<20	18[a]	10	3	<1	12	2
Y	2.0	2.4	<1	<1	2.4	3.6	1.3	0.8	3.0	1.8	0.4	0.8	1.0	2.9	1.6	0.8	1.4	3.7	4.1
Zn	31700	44900	69100	28300	15300	11900	30700	20606	7060	7310	20704	11779	10986	24500	18400	12400	190	27200	0
$\delta^{34}S$ [‰ CDT]	27.8	27.3		25.6	22.9		23.3	21.8	21.5	23.2	20.8	21.7	23.9	24.3	21.8		26.6	27.4	25.0
$^{206}Pb/^{204}Pb$	17.95	17.85		17.96	18.02		17.90		17.92	17.89				17.95					
$^{207}Pb/^{204}Pb$	15.84	15.74		15.84	15.83		15.80		15.71	15.76				15.83					
$^{208}Pb/^{204}Pb$	38.36	38.13		38.59	38.66		38.37		38.50	38.47				38.53					

Samples are from drill core KH026, from dumps and mine stopes (2, 3 and 5 levels).
Analyses were performed using ICP-MS and INAA (ActLabs, Canada) and by XRF (BGR).
[a] Analyses by XRF (BGR). Precision for S-isotopes is better than 0.7‰ on lab standards. Relative standard deviation for Pb isotope ratios is between 0.3% and 0.9%.

XRF data of the drill core can be obtained from the authors upon request.

Sulfide ores from Khusib Springs are exceptionally metal-rich, containing between 20% and 45% combined (Cu+Pb+Zn). Copper (7.5 to 41.3 wt.%) is the most abundant metal, with elemental Cu/(Cu+Zn+Pb) ranging from 0.73 to 0.94 in massive ore. Lead (0.2 to 5.1 wt.%) and Zn concentrations (0.7 to 6.9 wt.%) systematically change within drill core KH26, with Pb increasing and Zn decreasing towards depth. The ores are highly arsenian (6.5 to 14.7 wt.% As), and also contain up to 1.8 wt.% Sb. Molar As/(As+Sb) ranges from 0.92 to 0.99. The variations of metal concentrations in the orebody are illustrated in Fig. 6.

Minor elements in sulfide ore in appreciable amounts are Ag (434 to 3350 ppm, average of 22 samples: 1213 ppm), Cd (36 to 1089 ppm, average 104 ppm), and Se (18 to 237 ppm, average 87 ppm). Germanium concentrations (XRF data) range from 13 to 203 ppm (Figs. 3 and 6) and average to 92 ppm ($n=10$). Occasional enrichment of other trace elements is documented by the following maximum values: Bi (128 ppm), Co (188 ppm), Ga (57 ppm), Hg (59 ppm), Mo (139 ppm), Sn (103 ppm), and W (159 ppm). The concentrations of Cr, Ni, In, Ta, Tl and V are low, and Au and PGE are below 10 ppb (Pd 2.3 to 5.6 ppb, Pt 0.7 to 1.3 ppb, $n=6$).

Sulfur isotope ratios of whole rock sample splits range from +20.8‰ to +27.8‰ (mean 23.5‰; Fig. 6). They show a general tendency towards decreasing values with depth in the drill core KH26. Heavier whole-rock sulfur isotope ratios correlate with high Zn–Cd–Mn–(Ag) suggesting dependence on the abundance of sphalerite. Galena shows an opposite behaviour.

In contrast to sulfur isotopes, Pb isotope ratios in sulfides do not vary with depth. However, they cluster

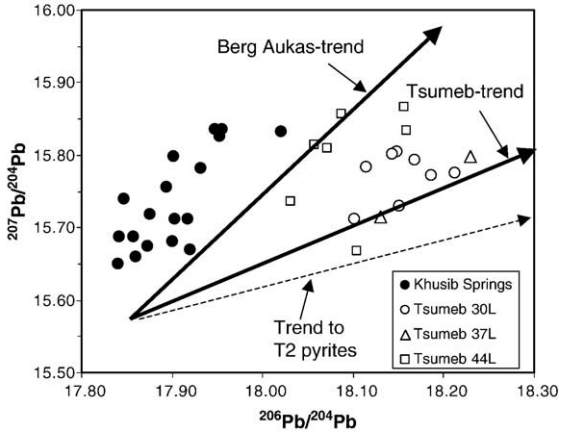

Fig. 7. Pb isotope data of sulfide ore from the Khusib Springs (including unpublished data from Ongopolo) and Tsumeb deposits (30, 37 and 44 levels). Trends established for Tsumeb- and Berg Aukas-type deposits are from Allsopp et al. (1981) and Hughes (1987). A trend pointing towards the composition of radiogenic pyrite in the lower Maieberg Formation (T2) in the footwall of the Khusib Springs deposit is also given.

at lower $^{206}Pb/^{204}Pb$, but similar $^{207}Pb/^{204}Pb$ and $^{208}Pb/^{204}Pb$ compared to ore samples from the Tsumeb deposit (Allsopp et al., 1981; Hughes, 1987; Kamona et al., 1999). In the past, linear Pb isotopic trends of ores from deposits in the OML have been interpreted to represent mixing of two or more components with distinct Pb isotopic signatures. Khusib Springs ores fall off the trends established for Berg Aukas and Tsumeb-type deposits and form a separate group (Fig. 7).

Low-grade ore intersected in an extensive breccia zone in drill core KH66 between 360 and 380 m depth (south-eastern extension of the massive orebody) carries up to 3% combined (Cu+Zn+Pb). Ratios between

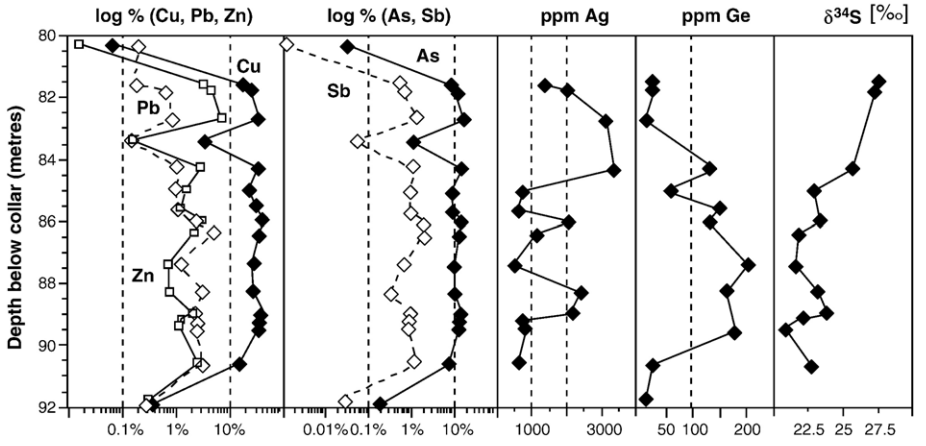

Fig. 6. Variation of the concentration of selected elements and of δ^{34} S in the orebody of drill core KH26, Khusib Springs.

base metals and semimetals (As, Sb) are similar to massive ore, although Zn is more abundant than Pb. Concentrations of trace elements are overall low: Ag <134 ppm, Cd <92 ppm, and Ge <1 ppm ($n=3$, total digestion ICP-MS). δ^{34}S varies from to 23‰ to 27‰. In contrast to massive ore, the disseminated footwall mineralization sampled in the mine has high concentrations of Zn (11 to 27 wt.%) at moderate Cu (1620 to 1920 ppm), Pb (145 to 347 ppm) and As (426 to 628 ppm). Concentrations of Ag (average: 26 ppm), Sb (22 ppm), Se (11 ppm) and Ge (<0.2 ppm) are low (Table 2). δ^{34}S is close to 25‰, which is within the range measured in massive sulfide ore.

Concentrations of non-metallic elements in the ore largely depend on the amount of carbonate gangue. The latter is dominated by dolomite in most samples, with CaO/MgO averaging 1.5. Barium concentrations are low (<100 ppm), and Sr (8 to 90 ppm) correlates negatively with MgO.

In sulfide ore, germanium has significant positive correlations (Spearman rank correlation, significance >80%) with Tl, S, Cu, As, Sb, Co, Al, and negative correlations with Ca, Sr, Mn, Mg and Y (in decreasing significance). Varimax factor analysis was carried out on 22 massive sulfide ore samples (Table 3), using the total digestion ICP-MS data for Ge. Three major and two less significant factors dominate about 90% of the total variance. Factor 1, which is statistically the most significant (44.7%), contains two groups of elements: Ge, S, Cu, As, Co represent the Cu–As-rich sulfide ore (tennantite–enargite); negative loadings for Sr, Mg, Ca, and Mn reflect the carbonates within the gangue (host rock and hydrothermal carbonates). Factor 2 consists of Zn, Cd, Hg, Ag, Sb, and is interpreted as a sphalerite and Ag sulfide factor; germanium has a significant negative loading in factor 2. Factor 3 combines Pb, Se and Sb (galena). Factor 4 comprises Al and K, and is interpreted to reflect the white mica and clay mineral fraction; a weak loading of Ge in this factor is noteworthy. Factor 5 is represented by Fe (correlating with Bi and Ni) and attributed to pyrite. The presence of Ge in more than one factor reflects the chalcophile and lithophile geochemical behavior of the element.

5. Microanalysis by μ-XRF

Several drill core slabs and polished sections were qualitatively analyzed using an X-ray microscope (ITRAX, COX Analytical Systems; Oberthür et al., 2000). The instrument is equipped with a Röntec Si(Li) detector and a Mo long fine focus XRD-tube (Philips). Operating conditions were 45 kV acceleration voltage, 30 mA, and 0.5 s time per spot. Samples were scanned in 100 μm steps, and up to 50 elements (in the parts per million to percent range) were simultaneously and semiquantitatively analyzed. The results are displayed in Fig. 4 as colored element distribution images either with gradual, but non-linear increase in concentration (due to mathematical data manipulation such as multiplication and filtering), or as overlays of up to three element patterns.

Fig. 4A shows a laminated dolomite (exemplified by the Ca distribution map, Fig. 4Ab) from the uppermost part of the orebody containing bedding-parallel, 1 to 2 cm thick massive sulfide layers. Copper-rich ore layers (Fig. 4Ab) have homogeneous concentrations of Cu and Zn due to dominant tennantite. Iron enrichment (Fig. 4Ab) is related to pyrite clouds mainly at the margins of sulfide layers towards dolomite and as infiltrations into the dolomite. Lead (Fig. 4Ac) is concentrated as galena mainly along the ore layer margins and forms large crystals along a vug filled with manganiferous calcite. Elevated intensities for Ge (Fig. 4Ac) in calcite vugs are probably related to reflection phenomena from large calcite crystals. However, combination of Zn and Ge (violet color) reflects the asso-

Table 3
Varimax factor analysis scores (oblique solution primary pattern matrix) from whole-rock geochemical data for 22 samples of sulfide ore from Khusib Springs

Factor 1 (+)	Factor 1 (−)	Factor 2 (+)	Factor 2 (−)	Factor 3	Factor 4	Factor 5
44.7%		19.1%		13.9%	6.5%	5.3%
Ge (1.0)	Sr (1.0)	Zn (1.0)	Ge (0.63)	Se (0.98)	Al (0.98)	Fe (0.88)
S (0.97)	Mn (0.96)	Cd (1.0)		Pb (0.95)	K (0.96)	
Cu (0.91)	Mg (0.96)	Hg (0.73)		Sb (0.50)	Ge (0.40)	
As (0.83)	Ca (0.95)	Ag (0.62)				
Co (0.65)		Sb (0.58)				

Samples are from drill core KH026, from dumps and mine stopes (2, 3 and 5 levels).
The five strongest factors are given, contributing 90% to the total variance. Factors 1 and 2 consist of two groups of elements, each with positive and negative loadings. Proportions of the data variance contributed by each factor are indicated in percent.

ciation of Ge-bearing minerals (colusite) with sphalerite at the lower dolomite/ore contact (see also Fig. 5b).

An example of texturally complex massive Cu ore replacing laminated dolomite is illustrated in Fig. 4B. Classified (non-linear) Cu concentrations (Fig. 4Bc) indicate that the ore layer in the central part of the image is composed of enargite (green colors) replaced by chalcocite-group minerals having higher Cu concentrations (Fig. 4Bc). In the upper and lower layers, tennantite that replaces enargite, and pyrite predominate. Lead concentrations are low in the bulk of the ore, but are higher towards the margins, with highest concentrations (as large galena crystals) in calcite vugs (Fig. 4Bb). Intensities on Ge (Fig. 4Bb) are high mainly in calcite (reflection from crystal planes?); however, Ge concentrations are also elevated in narrow irregular vein-type structures in the sulfide ore, which are clearly visible at higher magnification only. Such structures are identified as former stylolites where Ge-bearing colusite has precipitated.

Fig. 4C shows an example of breccia ore, which is common in the lower part of the drill core. The classified Fe intensity map (Fig. 4Cb) is grouped into five intensity windows, which correspond to different phases in the ore. Pyrite makes up about 8.9% of the area (yellow colors, highest intensities). Green, violet and blue colors are attributed to different generations of carbonates, including primary dolomite clasts (dark blue) and secondary vugs filled with Fe-bearing calcite and/or ankerite (green). Calcite veins/vugs in clasts and ore are slightly enriched in Fe (light blue).

The combination of optical scans and X-ray maps illustrates the texturally complex character of the Khusib Springs orebody. Classified element distribution images can be used to map the major ore minerals (Fig. 4B, C), and element overlay images help to identify phases of interest. Although concentrations of trace elements such as Ge are in the parts per million range only, zones of enrichment can be localized (Fig. 4A, B).

6. Mineral chemistry

More than 700 quantitative wavelength dispersive analyses were performed on polished sections using a CAMECA SX100 electron microprobe (EMP) equipped with five wavelength-dispersive spectrometers. Representative analyses of important minerals are presented in Table 4. Analytical conditions for the routine analysis of sulfides were: 20 kV acceleration voltage, 20 nA beam current, and measurement time 10 to 20 s on peak. Element standards were used for the following X-ray lines: V Kα, Mn Kα, Co Kα, Ni Kα, Cu Kα, Ge Kα, Se Lα, Mo Lα, Ag Lα, Cd Lα, Sn Lα, and W Lα. Mineral standards were used for S Kα and Zn Kα (sphalerite), Fe Kα (pyrrhotite), Ga Kα and As Lα (GaAs?), Sb Lα (antimonite), Hg Lα (cinnabar), and Pb Mα (galena). Detection limits range from 300 ppm (Mn, Co, Ni) to 2000 ppm (Hg, W). Silicates and carbonates were measured at 15 kV, 10 nA and calibrated using biotite (Si, Al, Mg, Fe, K), kaersutite (Ca, Ti), albite (Na), rhodonite (Mn), barite (Ba), tugtupite (Cl) and fluorite (F) as standards.

Conditions for EMP trace element analysis in sulfides and silicates were: 30 kV acceleration voltage, 200 to 300 nA beam current, measurement time 200 s on peak; detection limits (2σ) achieved using this set-up were 30 ppm for Ge, Ga, Fe and Ag, and 90 ppm for Cd. In order to verify the EMP trace analytical data, the concentrations of Ge, Ga and Ag were determined in enargite and tennantite separated from a sulfide ore from Khusib Springs (KS-03) using secondary ion mass spectrometry (SIMS) (S. Chryssoulis, AMTEL, Canada). The analyses were performed on a polished grain mount with particles in the 150 to 212 μm size range. A cesium (Cs^+) primary beam was used for Ge and Ag, and an oxygen (O^-) beam was used for Ga. The primary beam current was 20 nA, the primary accelerating voltage was 10 keV, and the impact energy was 14.5 keV. The diameter of analysis was in the range of 30 to 40 μm at a depth of 0.3 to 1 μm; counting time was 5–10 s, and mean detection limits achieved were 2 to 5 ppm for Ge, 0.02 to 0.1 ppm for Ga, and 0.05 to 0.4 ppm for Ag. Quantification relied on mineral specific implants of each element using the approach described by Chryssoulis et al. (1989). Details and results for three further sulfide ore samples from the Otavi Mountain Land will be published elsewhere.

6.1. Ge-bearing minerals

6.1.1. Colusite

Ge-bearing colusite [$Cu_{26}V_2(As,Ge)_6S_{32}$], which was identified as small (usually <50 μm, up to 100 μm) subhedral or anhedral single crystals in most drill core samples downhole from 82.7 m (Figs. 3 and 5a, b), is the most abudant mineral carrying Ge as a major element at Khusib Springs. Compared to enargite, the mineral has a slight but distinct brownish-rose color in reflected light, but otherwise its reflection behavior is similar. Many colusite grains are optically and chemically inhomogeneous. Their composition best fits to a Ge-bearing variety of colusite, with Ge/(Ge+As) ranging from 0.14 to 0.47 ($n=88$). Germanium and arsenic display a perfect negative correlation. Apart

Table 4
Representative electron microprobe analyses of sulfide minerals from Khusib Springs

Mineral	Colusite	Colusite	Colusite	Colusite	Germanite	Stannoidite	Tennantite	Tennantite	Ag–Tn	Tetrahedrite	Enargite	Enargite	Sphalerite I	Sphalerite II	Sphalerite III	Pearceite	Pearceite
Sample (Analysis)	AS6461 (21)	AS6459 (27)	AS6454b (13)	AS6648 (14)	KS-03(61)	KH75.8 (9)	KH92.7 (3)	AS6459 (3)	AS6461 (43)	AS6593 (9)	KH92.7 (2)	AS6456 (13)	AS6653 (7)	AS6454a (1)	AS6456 (1)	AS6459 (21)	AS6593 (16)
(wt.%)																	
S	30.49	32.32	31.54	31.07	30.63	29.52	27.83	27.69	25.62	25.07	32.84	32.60	33.37	33.06	31.92	19.04	17.83
V	1.48	2.36	3.10	2.42	0.04	<mdl	<mdl	<mdl	0.01	<mdl	0.01	0.01	<mdl	0.01	<mdl	0.02	<mdl
Mn	<mdl	<mdl	<mdl	0.03	na	<mdl	0.00	<mdl	<mdl	<mdl	<mdl	<mdl	<mdl	0.31	<mdl	<mdl	<mdl
Fe	1.16	0.35	0.30	0.26	3.45	9.04	0.62	0.85	0.13	0.01	0.03	0.03	1.20	0.02	0.07	0.05	0.01
Co	0.01	0.01	<mdl	<mdl	na	<mdl	<mdl	<mdl	0.01	<mdl	0.01	<mdl	<mdl	<mdl	<mdl	<mdl	<mdl
Ni	<mdl	<mdl	<mdl	<mdl	na	<mdl	<mdl	<mdl	<mdl	<mdl	0.01	<mdl	<mdl	0.01	0.02	0.01	<mdl
Cu	49.38	50.81	50.14	48.43	47.12	40.28	49.22	43.70	48.32	39.53	49.83	49.43	0.04	0.10	1.60	29.06	21.54
Zn	0.33	0.10	0.01	1.41	0.31	4.40	2.11	7.12	5.52	8.55	0.03	<mdl	66.61	66.59	63.53	<mdl	0.28
Ga	0.01	<mdl	0.01	<mdl	<mdl	0.02	<mdl	<mdl	<mdl	<mdl	<mdl	0.01	<mdl	0.06	<mdl	0.02	<mdl
Ge	5.17	3.01	3.87	4.20	8.08	0.68	0.25	<mdl	<mdl	0.02	0.44	0.07	<mdl	0.02	<mdl	<mdl	0.06
As	6.89	10.88	9.39	5.96	4.47	0.03	19.71	15.77	15.55	0.37	18.36	18.60	0.02	0.04	0.03	7.61	5.86
Se	0.12	<mdl	0.04	0.05	0.15	0.03	0.06	0.04	0.08	0.01	0.06	0.05	0.02	0.03	<mdl	<mdl	0.06
Mo	0.10	0.05	0.02	0.41	0.98	0.06	<mdl	0.11	0.07	0.02	0.15	0.13	0.10	0.12	0.16	0.04	<mdl
Ag	0.13	<mdl	0.05	<mdl	0.04	<mdl	0.31	0.24	5.27	0.37	0.10	0.21	0.01	0.02	0.93	45.24	53.06
Cd	<mdl	0.01	<mdl	<mdl	<mdl	0.01	0.04	0.07	0.01	<mdl	0.02	0.02	0.21	0.14	0.03	<mdl	0.09
Sn	0.17	0.05	0.24	4.44	na	17.76	<mdl	0.03	<mdl	0.09	0.01	0.01	0.02	0.02	<mdl	<mdl	<mdl
Sb	0.12	0.23	0.20	0.02	0.15	<mdl	0.38	5.82	0.11	27.36	0.07	0.15	<mdl	0.01	0.11	0.25	2.38
W	4.66	0.06	0.11	2.57	5.42	<mdl	<mdl	<mdl	<mdl	<mdl	<mdl	0.04	<mdl	<mdl	<mdl	<mdl	0.03
Hg	<mdl	0.01	0.02	<mdl	na	<mdl	0.61	0.02	<mdl	<mdl	<mdl	<mdl	<mdl	<mdl	<mdl	<mdl	0.05
Pb	<mdl	<mdl	<mdl	<mdl	na	<mdl	<mdl	<mdl	1.24	0.14	<mdl	<mdl	<mdl	<mdl	0.18	<mdl	<mdl
Total	100.22	100.25	99.04	101.26	100.85	101.83	101.14	101.47	101.92	101.52	101.96	101.37	101.60	100.53	98.58	101.34	101.26
(at.%)																	
S	48.08	49.13	48.62	48.48	48.29	47.35	44.23	44.55	41.80	44.18	49.60	49.59	49.91	50.01	49.62	37.67	37.27
V	1.47	2.25	3.01	2.37	0.04	0.00	0.00	0.00	0.01	0.00	0.01	0.01	0.00	0.01	0.00	0.02	0.00
Mn	0.00	0.00	0.00	0.03	na	0.00	0.00	0.00	0.00	0.00	0.00	0.00	0.00	0.27	0.00	0.00	0.00
Fe	1.05	0.31	0.27	0.23	3.12	8.32	0.56	0.78	0.13	0.01	0.03	0.02	1.03	0.02	0.06	0.06	0.01
Co	0.01	0.01	0.00	0.00	na	0.00	0.00	0.00	0.01	0.00	0.01	0.00	0.00	0.00	0.00	0.00	0.00
Ni	0.00	0.00	0.00	0.00	na	0.00	0.00	0.00	0.00	0.00	0.01	0.00	0.00	0.00	0.02	0.01	0.00
Cu	39.28	38.96	38.99	38.12	37.47	32.59	39.47	35.47	39.78	35.15	37.97	37.94	0.03	0.07	1.25	29.01	22.72
Zn	0.26	0.08	0.00	1.08	0.24	3.46	1.65	5.62	4.41	7.39	0.02	0.00	48.85	49.39	48.42	0.00	0.29
Ga	0.01	0.00	0.01	0.00	0.00	0.01	0.00	0.00	0.00	0.00	0.00	0.01	0.00	0.04	0.00	0.02	0.00
Ge	3.60	2.02	2.63	2.89	5.63	0.48	0.18	0.00	0.00	0.01	0.29	0.05	0.00	0.01	0.00	0.00	0.05
As	4.65	7.07	6.20	3.98	3.02	0.02	13.40	10.86	10.86	0.28	11.87	12.11	0.01	0.02	0.02	6.44	5.25
Se	0.08	0.00	0.02	0.03	0.10	0.02	0.04	0.03	0.05	0.01	0.04	0.03	0.01	0.02	0.00	0.00	0.05
Mo	0.05	0.02	0.01	0.21	0.52	0.03	0.00	0.06	0.04	0.01	0.07	0.07	0.05	0.06	0.09	0.03	0.00
Ag	0.06	0.00	0.02	0.00	0.02	0.00	0.15	0.12	2.56	0.19	0.04	0.09	0.00	0.01	0.43	26.61	32.97
Cd	0.00	0.00	0.00	0.00	0.00	0.00	0.02	0.03	0.01	0.00	0.01	0.01	0.09	0.06	0.01	0.00	0.05
Sn	0.07	0.02	0.10	1.87	na	7.69	0.00	0.01	0.00	0.04	0.00	0.00	0.01	0.01	0.00	0.00	0.00
Sb	0.05	0.09	0.08	0.01	0.06	0.00	0.16	2.46	0.05	12.70	0.03	0.06	0.00	0.00	0.05	0.13	1.31
W	1.28	0.02	0.03	0.70	1.49	0.00	0.00	0.00	0.00	0.00	0.00	0.01	0.00	0.00	0.00	0.00	0.01
Hg	0.00	0.00	0.01	0.00	na	0.00	0.15	0.01	0.00	0.00	0.00	0.00	0.00	0.00	0.00	0.00	0.02
Pb	0.00	0.00	0.00	0.00	na	0.00	0.00	0.00	0.31	0.04	0.00	0.00	0.00	0.00	0.04	0.00	0.00

Note:<mdl=below detection limit; na=not analysed.

from the major components Cu (average ± standard deviation: 50.3 ± 1.0 wt.%), V (2.9 ± 0.5 wt.%), Ge (4.0 ± 0.8 wt.%), As (9.0 ± 1.3 wt.%) and S (31.5 ± 0.5 wt.%), the following elements were detected in minor amounts (in wt.%): Fe (0.62 ± 0.66), Zn (average: 0.41), Se (to 0.15), Mo (to 2), Ag (to 2.4), Sn (to 5.1), Sb (to 2.0), and W (to 4.8; average 0.76) (Table 4, Fig. 8a, b). Many colusite grains produce inhomogeneous backscatter electron images due to locally elevated W concentrations (Fig. 5a, b). Such areas are either patchy-irregular, lamellar or follow growth zones outlining crystal faces; they have lower V contents than stoichiometric colusite. Tungsten correlates positively with Ge and negatively with V and As concentrations (Fig. 8a). Tin concentrations are lower than 0.5 wt.% in most grains analyzed, except for disseminated tennantite aggregates in coarse hydrothermal dolomite, where colusite was found to contain 1.3 to 5.1 wt.% Sn (Table 4; Fig. 8a).

6.1.2. Germanite

Germanite was identified only in the grain mount prepared for SIMS analysis (KS-03). The small grains form composite inclusions (<30 μm in size) in tennantite with Ge- and W-bearing colusite and tungstenite. Two analyses reveal the following composition (in wt.%): Cu 47.1 to 49.0, Fe 3.4 to 4.2, Ge 7.2 to 8.1, As 4.5 to 5.6, W 2.2 to 5.4, S 30.6 to 30.8 (Table 4). Minor concentrations of Zn (0.3 wt.%), Sb (0.2 wt.%) and Sn (0.06 to 0.07 wt.%) are detected.

6.1.3. Stannoidite

Stannoidite [$Cu_{8.1-8.4}(Fe,Zn)_3Sn_{1.9-2.0}S_{12}$] was detected as small (20 μm) euhedral inclusions of brownish-orange color along with pyrite in tennantite patches, some 5 m stratigraphically above the main orebody (Figs. 3 and 5c). Germanium concentrations range from 0.5 to 0.7 wt.% (Table 4).

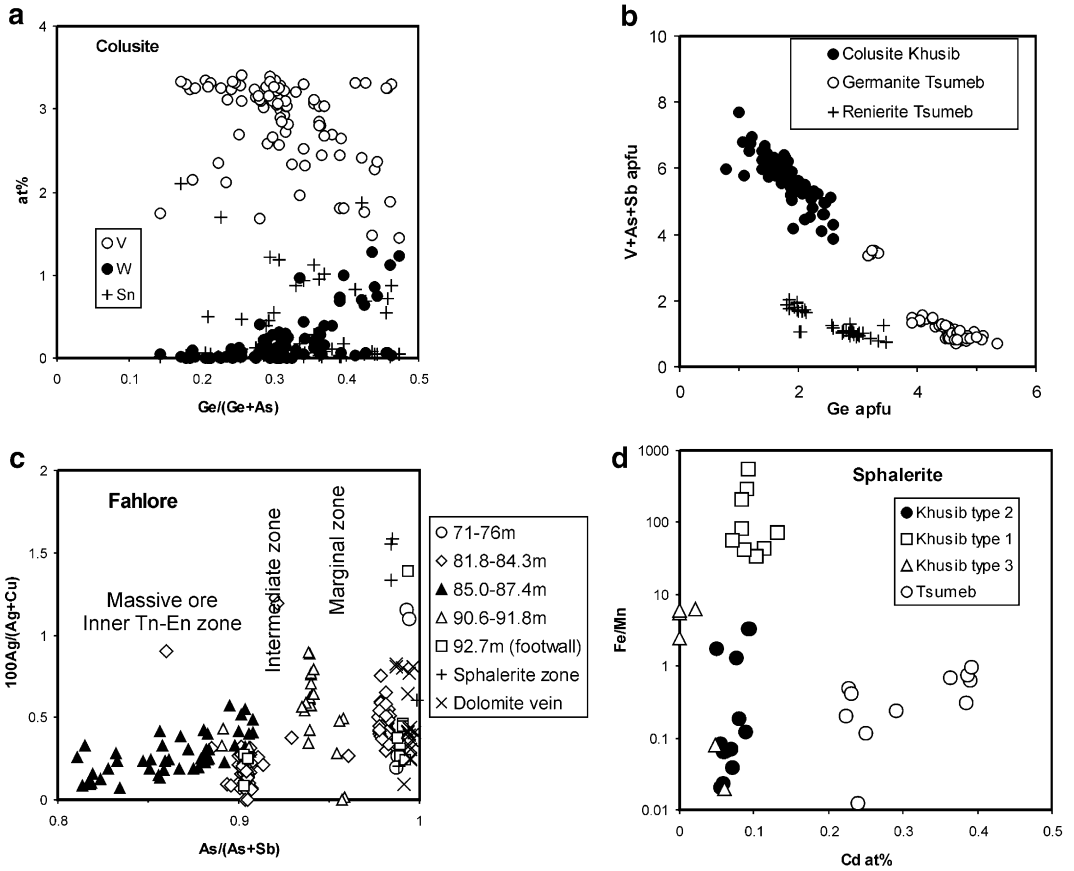

Fig. 8. Mineral chemistry: (a) Molar Ge/(Ge+As) versus V, W and Sn (in at.%) in colusite, (b) Diagram of atoms Ge pfu (calculated to 32 sulfur atoms) versus ∑V+As+Sb in Ge-bearing colusite from Khusib Springs, compared to germanite and reniérite from Tsumeb, (c) Molar As/(As+Sb) versus 100*Ag/(Cu+Ag) in As-rich fahlore. Fahlore compositions change from Sb-rich, Ag-poor in the central orebody towards more As- and Ag-rich fahlore in contact with carbonate host rocks and in the marginal ore. (d) Molar Fe/Mn versus Cd (at.%) in sphalerite from the Khusib Springs and Tsumeb deposits.

6.1.4. Fahlore

Zinc-rich tennantite (on average 7.2 wt.% Zn, range 1.8 to 9.5 wt.%, $n=285$) is the major sulfide mineral in the Khusib Springs deposit (Fig. 3). Chemically, it is characterized by molar As/(As+Sb) ratios ranging from 0.77 to 0.99, Fe/(Fe+Zn) from 0.01 to 0.67, and 100*Ag/(Ag+Cu) from 0 to 1.6 (Fig. 8c). Averages and standard deviations of fahlore compositions from all samples investigated are presented in Table 5. Compared to fahlore from the Tsumeb deposit, average Khusib fahlore carries higher concentrations of Mn (0.1 wt.% on average in the central part of the ore), Sb and Ag (Table 6). Silver averages 0.27 wt.% in ordinary tennantite but may reach up to 1 wt.%, thus making tennantite the major carrier of Ag in the deposit. Silver increases with increasing As/(As+Sb) ratio of the fahlore (Fig. 8c), in contrast to the general tendency of higher Ag contents in Sb-rich fahlores (Ebel and Sack, 1991).

Within individual samples, fahlores are homogeneous in terms of As–Sb ratio (Fig. 8c; Table 5), but in some samples they are overgrown by Sb-rich fahlore (tetrahedrite). In the orebody, fahlore compositions change from rich in As–Fe–Ag in the hanging-wall, to more Sb-rich and Ag-poor in the central part, to As- and Zn-rich, but Ag- and Fe-poor in the footwall (Figs. 3 and 8c; Table 5). Their average As/(As+Sb) ratios are closely correlated with the respective whole rock As/Sb value. Zn-poor tennantite (<3 wt.% Zn) was observed as a minor constituent intergrown with enargite in dolomite veins in the footwall of the orebody (KH26/92.7 m), carrying considerable Ge (to 0.26 wt.%), Ag (0.3 wt.%) and Hg (0.3 to 0.7 wt.%) (Fig. 5g; Tables 4 and 5).

Thin (several μm) rims of growth-banded Sb-rich fahlore (tetrahedrite with As/(As+Sb)=0.02 to 0.29) occur at contacts of tennantite with galena and enargite, often growing into open vugs (Fig. 5d), and are also associated with pearceite–polybasite, sphalerite and digenite. Significant Ag (0.49 wt.% on average) and Pb (0.34 wt.%) are detected (Table 4). Fahlores intermediate between tennantite and tetrahedrite with As/(As+Sb)=0.55 to 0.62 occur in similar textural positions.

Germanium concentrations in fahlore are mostly below the detection limit of the routine analytical EMP method (<800 ppm). Trace analyses using EMP in several samples revealed between 40 and 110 ppm Ge in a few grains only; most grains analyzed have less than 30 ppm Ge. SIMS analyses of 12 tennantite grains in sample KH03 gave 112 ± 10 ppm Ge and 48 ± 4 ppm Ga (Table 6). EMP trace analyses on the same grains gave much lower Ge concentrations of 11 ± 9 ppm Ge (maximum 23 ppm), and 42 ± 10 ppm Ga. Silver concentrations in this particular sample range from 160 to 793 ppm and average 447 ± 180 ppm Ag ($n=16$, EMP).

6.1.5. Enargite

Enargite occurs both as anhedral inclusions several 100 μm in size in tennantite or as a matrix phase and is frequently associated with galena, pyrite, digenite, and locally pearceite–polybasite and chalcopyrite (Fig. 5e–h). Considerable concentrations of Ag (0.21 ± 0.18 wt.%) and Sb (0.26 ± 0.13 wt.%) are noteworthy (Table 4). Elevated Ge concentrations occur in enargite within mineralized dolomite veinlets associated with Ge-bearing tennantite (Fig. 5g; Table 4) and in marginal portions of sulfide laminae associated with Ge-bearing colusite.

Trace element determinations reveal a wide range of Ge concentrations from <40 ppm to 4350 ppm (Table 6). SIMS and trace EMP analyses were carried out on the same grains of sample KS-03. Averages, standard deviations and maximum concentrations for 17 grains correspond well for Ge: SIMS, 566 ± 406 (121 to 1558 ppm), EMP, 484 ± 452 (17 to 1686 ppm) (Table 6). SIMS element maps reveal comparatively homogeneous Ge distributions within single enargite grains. Gallium concentrations are low (SIMS: 1.4 ± 2.4 ppm, maximum 7.5 ppm). The concentrations of Ag are highly variable (SIMS, 13 to 6415 ppm; EMP,<10 to 7721 ppm), probably indicating the presence of small Ag-rich inclusions.

6.2. Other ore minerals

Sphalerite is restricted to the upper parts and the footwall of the orebody. In the footwall, a prominent zone of disseminated (0.5 to 1 cm in size) sphalerite ± chalcopyrite ± galena ± pyrite is developed. Based on chemical data and textural observations, three sphalerite types are distinguished (Fig. 8d). Sphalerite I is restricted to disseminated ore in the footwall; it is enriched in Fe (0.7 to 1.2 wt.%), carries 0.2 to 0.3 wt.% Cd, but low concentrations of Cu and Mn (Tables 4 and 6). Sphalerite II occurs in massive Cu ore, is low in Fe, but carries Mn (0.2 to 0.4 wt.%), Cd (up to 0.2 wt.%) and Cu (0.1 to 0.5 wt.%). Trace element analyses give <30 to 3000 ppm Fe, 700 to 900 ppm Ga, <30 ppm Ge, <30 to 68 ppm Ag, and 1440 to 1793 ppm Cd. Sphalerite III (Fig. 5d) is partly collomorphous ("schalenblende"). According to EMP analysis this type is rich in Cu (1 to 3 wt.%) and Ag (0.1 to 1.8 wt.%), carries some Sb

Table 5
Fahlore compositions (**average** and standard deviation in wt.%; molar ratios) of N analyses from drill core KH26, mine and ore dump samples at Khusib Springs

Sample	Depth (KH26)	S	Mn	Fe	Cu	Zn	Ga	Ge	As	Se	Mo	Ag	Cd	Sb	Pb	100*As/(As+Sb)	100*Fe/(Zn+Fe)	10^5*Ag/(Cu+Ag)	N
KH26/71.0	71.0	**28.23**	**<mdl**	**1.46**	**44.04**	**6.96**	**<mdl**	**<mdl**	**19.83**	**0.03**	**0.03**	**0.20**	**0.02**	**0.41**	**<mdl**	**98.8**	**19.8**	**27**	3
		0.23		0.02	0.18	0.04			0.03	0.02	0.03	0.06	0.02	0.01		0.0	0.3	7	
KH26/75.8	75.8	**28.15**	**<mdl**	**2.67**	**44.20**	**5.55**	**0.010**	**<mdl**	**20.07**	**0.06**	**0.01**	**0.85**	**0.04**	**0.20**	**<mdl**	**99.4**	**36.1**	**112**	3
		0.13		0.05	0.32	0.03	0.002		0.05	0.06	0.02	0.03	0.02	0.02		0.1	0.5	3	
AS6453	81.8	**28.02**	**0.12**	**0.35**	**43.68**	**8.12**		**0.010**	**19.67**			**0.35**	**0.06**	**0.63**	**0.07**	**98.1**	**4.8**	**47**	38
		0.23	0.03	0.11	0.43	0.37		0.021	0.19			0.06	0.02	0.06	0.04	0.2	1.6	8	
AS6454a	82.7	**28.01**	**0.13**	**0.31**	**43.79**	**8.21**	**0.022**	**0.044**	**19.50**	**0.03**	**0.20**	**0.46**	**0.05**	**0.62**	**<mdl**	**98.1**	**4.3**	**61**	3
		0.14	0.03	0.21	0.54	0.36	0.021	0.029	0.04	0.03	0.16	0.09	0.02	0.05		0.2	3.0	13	
AS6593 type I	83.4	**27.98**	**0.17**	**0.78**	**45.79**	**6.97**	**0.039**	**0.013**	**19.11**	**0.04**	**<mdl**	**0.21**	**0.05**	**1.27**	**0.03**	**96.1**	**11.6**	**27**	1
AS6593 type II	83.4	**26.95**	**<mdl**	**0.07**	**45.39**	**7.62**	**<mdl**	**<mdl**	**16.25**	**0.05**	**0.07**	**0.70**	**<mdl**	**4.31**	**0.36**	**86.0**	**1.0**	**90**	1
AS6455	84.3	**27.75**	**0.11**	**0.77**	**42.26**	**6.46**		**0.009**	**17.29**			**0.14**	**0.05**	**2.98**	**0.08**	**90.4**	**12.2**	**19**	66
		0.29	0.04	0.15	1.95	0.56		0.015	0.38			0.12	0.02	0.18	0.11	0.5	2.3	15	
AS6456	85.0	**27.81**	**0.15**	**0.84**	**43.86**	**6.73**	**0.014**	**<mdl**	**17.58**	**0.02**	**0.05**	**0.32**	**0.05**	**3.07**	**0.08**	**90.3**	**12.7**	**43**	10
		0.17	0.01	0.23	0.52	0.10	0.011		0.59	0.02	0.05	0.07	0.02	0.10	0.24	0.4	3.0	10	
AS6595	85.6	**27.72**	**0.05**	**1.28**	**44.22**	**6.67**	**0.015**	**0.016**	**16.76**	**0.02**	**0.05**	**0.17**	**0.06**	**4.45**	**<mdl**	**85.9**	**17.5**	**22**	7
		0.39	0.05	0.84	0.70	0.19	0.017	0.023	0.16	0.02	0.04	0.07	0.01	0.13		0.4	9.5	9	
AS6457	86.0	**27.63**	**0.25**	**0.55**	**44.73**	**7.21**	**0.011**	**0.001**	**17.03**	**0.03**	**0.05**	**0.20**	**0.06**	**4.24**	**<mdl**	**86.7**	**8.1**	**26**	18
		0.19	0.02	0.03	0.88	0.07	0.015	0.004	0.52	0.02	0.06	0.05	0.02	0.75		2.4	0.4	6	
AS6459	86.4	**27.61**	**0.08**	**0.58**	**43.92**	**7.34**	**0.009**	**0.010**	**15.91**	**0.02**	**0.05**	**0.12**	**0.06**	**5.95**	**<mdl**	**81.3**	**8.4**	**16**	8
		0.23	0.10	0.13	0.30	0.09	0.013	0.019	0.47	0.02	0.05	0.07	0.02	0.55		1.9	1.8	9	
AS6454b	87.4	**27.45**	**0.06**	**0.38**	**45.00**	**6.82**	**0.005**	**0.002**	**16.40**	**0.01**	**0.08**	**0.20**	**0.06**	**4.29**	**<mdl**	**86.1**	**5.9**	**26**	5
		0.21	0.10	0.20	1.10	0.56	0.007	0.004	0.70	0.01	0.06	0.10	0.01	0.47		1.7	2.7	12	
AS6461	90.6	**27.51**	**0.04**	**1.27**	**46.05**	**5.61**	**0.005**	**0.003**	**18.20**	**0.03**	**0.04**	**0.47**	**0.03**	**2.06**	**<mdl**	**93.5**	**20.7**	**59**	21
		0.67	0.05	0.40	0.88	0.18	0.008	0.008	0.54	0.02	0.04	0.13	0.01	0.54		1.7	5.8	17	
KH26/918	91.8	**28.27**	**<mdl**	**0.80**	**44.71**	**7.91**	**0.003**	**0.003**	**19.10**	**0.03**	**0.06**	**0.07**	**0.05**	**1.40**	**<mdl**	**95.7**	**10.6**	**10**	3
		0.24		0.02	1.11	0.22	0.006	0.006	0.07	0.03	0.04	0.12	0.01	0.08		0.2	0.2	16	
KH26/927	92.7	**28.11**	**<mdl**	**1.72**	**43.08**	**6.86**	**<mdl**	**0.026**	**18.21**	**0.07**	**0.10**	**0.06**	**0.03**	**3.18**	**<mdl**	**90.3**	**22.7**	**9**	3
		0.46		0.15	0.47	0.11		0.015	0.25	0.04	0.06	0.07	0.02	0.04		0.1	1.7	10	
KS-01	dolomite vug	**28.05**	**<mdl**	**1.45**	**43.15**	**7.18**	**<mdl**	**0.014**	**20.00**	**0.04**	**0.17**	**0.60**	**0.05**	**0.32**	**<mdl**	**99.0**	**19.2**	**81**	4
	(2 level)	0.50		0.04	0.11	0.08		0.016	0.04	0.03	0.10	0.01	0.01	0.15		0.5	0.6	1	
AS6648	dolomite vug	**28.07**	**<mdl**	**0.89**	**43.27**	**7.66**	**0.003**	**0.033**	**19.55**	**0.02**	**0.24**	**0.29**	**0.04**	**0.18**	**<mdl**	**99.4**	**11.9**	**39**	14
	(5 level)	0.24		0.21	0.42	0.35	0.007	0.069	0.49	0.02	0.26	0.12	0.02	0.04		0.1	2.9	16	
AS6652	footwall min.	**28.13**	**<mdl**	**3.54**	**42.75**	**4.67**	**<mdl**	**0.001**	**18.16**	**0.01**	**0.01**	**0.19**	**0.03**	**1.38**	**<mdl**	**93.6**	**47.1**	**33**	4
	(5 level)	28.28		3.61	43.01	4.74		0.033	19.21	0.07	0.22	0.31	0.05	2.70		2.2	0.2	9	
AS6653	footwall min.	**28.46**	**<mdl**	**4.49**	**43.33**	**4.46**	**0.005**	**0.011**	**20.07**	**0.04**	**0.19**	**0.84**	**0.02**	**0.41**	**0.02**	**98.8**	**55.2**	**112**	6
	(5 level)	0.18		1.65	0.35	2.51	0.010	0.014	0.16	0.03	0.07	0.43	0.02	0.18	0.03	0.5	20.9	58	
KS-03 (SIMS)	ore dump	**27.77**		**1.82**	**45.73**	**4.70**	**0.001**	**0.001**	**17.93**	**0.04**		**0.06**	**0.04**	**3.05**		**90.5**	**31.2**	**7**	18
		0.25		0.12	0.49	0.10	0.021	0.025	0.51	0.02		0.05	0.02	0.60		1.9	1.5	6	
AS5801	ore dump	**27.44**	**0.14**	**1.37**	**43.37**	**7.14**	**<mdl**	**<mdl**	**16.72**	**0.01**	**0.01**	**0.23**	**0.06**	**4.52**	**<mdl**	**85.7**	**17.9**	**31**	3
		0.10	0.08	0.75	0.82	0.15			0.32	0.02	0.02	0.05	0.02	0.04		0.3	8.2	7	
AS5799a	ore dump	**28.22**	**0.17**	**0.31**	**44.72**	**7.82**		**0.007**	**18.99**			**0.39**	**0.05**	**1.48**	**0.05**	**95.4**	**4.4**	**51**	12
		0.26	0.02	0.03	0.13	0.07		0.010	0.17			0.08	0.02	0.07	0.04	0.2	0.5	10	
AS5794b	ore dump	**27.74**	**0.14**	**0.30**	**43.57**	**7.71**		**0.012**	**17.09**			**0.09**	**0.04**	**3.80**	**0.07**	**88.0**	**4.4**	**12**	22
		0.24	0.07	0.18	1.29	0.43		0.020	0.68			0.10	0.02	0.81	0.04	2.6	2.8	13	
KH26/927 Ge	92.7	**27.80**	**0.01**	**0.58**	**48.92**	**2.28**	**0.002**	**0.200**	**19.37**	**0.03**	**0.07**	**0.40**	**0.04**	**0.31**	**<mdl**	**99.0**	**22.8**	**47**	8
		0.33	0.02	0.19	1.08	0.41	0.004	0.057	0.77	0.04	0.06	0.32	0.02	0.06		0.2	5.1	38	
Tetrahedrite	5 samples	**25.66**	**0.02**	**0.08**	**40.41**	**8.08**	**0.002**	**0.014**	**5.08**	**0.01**	**0.05**	**0.44**	**0.03**	**20.52**	**0.32**	**28.1**	**1.0**	**65**	13
		0.85	0.03	0.09	1.10	0.63	0.005	0.026	4.38	0.01	0.09	0.23	0.03	6.31	0.33	23.6	1.1	34	

<mdl = below mean detection limit.

Table 6
Composition of sulfide minerals in the Khusib Springs and Tsumeb deposits

Mineral	Location	Mn	Fe	Cu	Zn	Ga	Ge	**As**	Ag	Cd	Sb	Hg	Pb
Tennantite	Khusib	0.1	0.87	•	7.2	**50–90**	**<30–106**	•	0.27	0.05	2.4	0.03	0.04
	KS-03 IM					**48 ± 4**	**112 ± 10**						
	KS-03 TE					**48 ± 25**	**14 ± 22**		**447 ± 180**				
	Tsumeb*	0.003–0.04	0.1–1.2	•	6.6–8.6	**140–350**	**<30–135**	•	**150–3350**	0.14–0.23	0.2–1.4	<0.13	<0.1
	Tsumeb**		0.85	•	<9		**60–700**	•	**200–1800**	0.15	<0.49		
Enargite	Khusib	–	0.07	•	0.03	**<30**	**<30–4350**	•	0.21	<0.06	0.25	<0.2	<0.1
	KS–03 IM					**1.4 ± 2.4**	**556 ± 406**		**251 ± 301**				
	KS-03 TE					**1.7 ± 7.8**	**530 ± 397**		**479 ± 512**				
	Tsumeb*	<0.01	<0.3	•	<0.25	<0.02	**<270**	•	<0.17	<0.02	0.14	–	–
	Tsumeb**			•			**500**	•					
Sphalerite	Khusib I	0.007	0.79	0.14	•	**130**	**<30**	0.034	**<70**	0.22	<0.01	<0.2	<0.1
	Khusib II	0.24	0.8	0.31	•	**700–900**	**<30**	0.018	**<70**	0.16	<0.01	<0.2	<0.1
	Khusib III	0.04	0.03	1.79	•	**<30**	**<30**	0.028	0.91	0.02	0.08	0.01	0.29
	Tsumeb*	0.13	**<20–656**	0.45	•	**2000–3120**	**<30–68**	0.032	**<40**	0.57–0.88	<0.01	<0.1	<0.1
	Tsumeb**	<0.15	0.17–4.6	0.3	•	**490**	**70–140**			0.8–1.4		**<150**	
	OML***	<0.1	<2.55	0.01–0.3	•	**6–310**	**8–427**	**<179**	**87–219**	0.14–0.41	**16–136**		
Galena	Khusib	–	–	0.13	0.03	–	**–**	0.02	0.06	–	<0.01	<0.01	•
	Tsumeb*	–	–	<0.2	–	0.05	**–**	–	<0.06	–	–	–	•
	OML***	<0.014					**<70**		**42–599**		**26–432**		•
Pyrite	Khusib	<0.01	•	0.68	0.04	–	–	0.05	<0.01	<0.02	<0.01	<0.02	–
	Tsumeb*	<0.013	•	<1	<0.15	–	–	<0.01	<0.01	<0.01	<0.015	–	–
	Tsumeb**		•	<2				<7	**5–25**				
Digenite	Khusib	0.01	0.08	•	0.31	<0.01	0.01	0.05	1.1	0.01	<0.01	0.02	<0.1
	Tsumeb*	0.004	0.17	•	0.10	<0.01	<0.16	<0.04	0.17	0.01	<0.01	0.03	–

All values in wt.% except for numbers given in **bold** (in ppm). Quoted values represent averages and standard deviations (e.g. 0.11 ± 0.05), ranges (<30–100), or maximum values detected (e.g.<0.49).

IM = ion microprobe; TE = trace EPMA; *own data from sulfide ore at Tsumeb (30 and 37 Levels); **from Lombaard et al. (1986); *** Mineral concentrate data from ores in different deposits of the Otavi Mountain Land (OML; Emslie and Beukes, 1981); • = major component; – = below detection limit.

and Pb, but mostly lacks Mn, Fe, Cd (<100 ppm) and Ge (<30 ppm; Tables 4 and 6). "Schalenblende" is porous, usually altered to an even more Cu- and Ag-rich zinc sulfide along rims, and is associated with (Ag-bearing) chalcocite, tetrahedrite, pearceite–polybasite and galena (Fig. 5d). It occurs along fractures, typically at the interface between tennantite and enargite, or associated with Ge-bearing tennantite and enargite in mineralized dolomite veinlets. Sphalerite III and Sb-rich sulfosalts are late in the paragenetic sequence (Table 1).

Galena carries on average 0.17 wt.% Se and 0.13 wt.% Cu ($n=28$). Some elevated Ag concentrations correlate with elevated Cu, suggesting sub-microscopic inclusions of fahlore. A few trace element determinations give <40 ppm Ag. Along cleavage planes, galena may be altered to a phase having lower reflectance that contains as much as 4 wt.% Cu and 0.5 to 0.6 wt.% Ag.

In reflected light, tarnishing colors of some *pyrites* indicate zoning. In such cases, weak differences in the concentrations of minor elements (Ni, Co, Cu) are detected (e.g., cores richer in Cu, rims richer in Ni). In general, pyrite has low concentrations of Co and Ni averaging to only 0.038 and 0.034 wt.%, respectively. Maximum concentrations encountered are 0.64 wt.% for both elements. Copper concentrations average 0.7 wt.%; additional impurities are As (0.05 wt.% on average, max. 0.8 wt.%) and Zn (up to 0.33 wt.%) (Table 6).

Tungsten–molybdenum sulfides, probably members of a *tungstenite-molybdenite* solid solution series [WS_2–MoS_2], occur as minute (<5 μm) grains in association with Ge–colusite, germanite, pearceite, tennantite, pyrite and dolomite. Very fine molybdenite intergrown with tungstenite was described from some Tsumeb ores (Geier and Ottemann, 1970a). Solid solution between molybdenite and tungstenite is very rare in nature (Höll and Weber-Diefenbach, 1973; Barkov et al., 2000).

Chalcocite-group minerals (*digenite* [Cu_9S_5] and *djurleite* [$Cu_{1.94-1.97}S$], probably *anilite* [Cu_7S_4]) are found replacing tennantite and enargite (Fig. 5d, g). Their composition ranges from [$Cu_{1.7}S$] to [$Cu_{1.95}S$], with minor concentrations (in wt.%) of Fe (<1), Zn (<1.7), As (<0.29) and Ag (<4.6). Microprobe analyses of *covellite* reveal significant Ag contents (0.24 to 2.3 wt.% Ag).

Four discrete Ag-rich phases were observed at Khusib Springs: (1) Most common is *pearceite–polybasite* [$(Ag,Cu)_{16}(As,Sb)_2S_{11}$], a Ag-(30 to 64 wt.%) and Cu-rich (12 to 45 wt.%) sulfosalt carrying considerable As (4 to 8 wt.%) and Sb (0.1 to 8.2 wt.%) (Fig. 5e, f; Table 4). Grains measuring up to 0.5 mm in size are frequently associated with tetrahedrite and sphalerite III, but also occur in tennantite, enargite and galena. (2) *Argentian tennantite* (2 to 10 wt.% Ag) is present as small grains only, usually rimming enargite towards Ag-poor tennantite (Fig. 5e; Table 4). (3) *Stromeyerite* [CuAgS] forms small inclusions in chalcopyrite associated with galena in tennantite ore. (4) *Native silver* carries very low concentrations (<0.2 wt.%) of Cu, Zn, S and no detectable Au or Hg.

Rutile, which is commonly associated with colusite along the margins of sulfide laminae, was found to contain considerable Cu (0.4 to 0.6 wt.%), V (0.5 to 0.6 wt.%), some Zn, As, Pb and up to 0.64 wt.% W.

6.3. Carbonates and silicates

The composition of carbonates associated with the mineralization is rather uniform, consisting mainly of dolomite and rarely of calcite. Dolomite, showing bright red cathodoluminescence colors, is poor in Fe (usually less than 0.5 wt.% FeO) but carries considerable Mn (typically 0.5 to 1.5 wt.% MnO) (Gross and Vollbrecht, 2003). Cores of coarse dolomite crystals and fragments, however, may carry as much as 5.0 wt.% FeO. In the ore zone, Mn-rich luminescent dolomite overgrowths form the rims of brecciated Fe-rich dolomite fragments. Calcite is characterized by yellow luminescence and carries as much as 1 mol% $MnCO_3$.

Muscovite and small amounts of kaolinite (Fig. 5h) are the only sheet silicates detected in ore and host rock samples. Muscovite is present either as small isolated flakes (<20 μm) in the carbonate host, in marginal portions of the ore (up to 80 μm in their longest axis), or forms stylolite-like accumulations within ore and host rock (Fig. 5h). Two chemical groups can be distinguished based on their Mg-numbers (100*Mg/(Mg+Fe)) and Si contents (Fig. 9). One group with lower Si contents (6.1 to 6.6 atoms per formula unit) has higher concentrations of Fe (Mg-number 50 to 80), whereas Si-rich micas (6.5 to 6.9 atoms Si) are essentially Fe-free (Mg-number>90). Thus, white mica compositions clearly follow a Tschermak substitution trend to phengite. Concentrations of F correlate with Si and reach up to 1 wt.% in the Mg-rich phengites. Such micas are closely associated with sulfide ore, whereas the Fe-bearing muscovite is more abundant in the host rock and in stylolites. In addition to high Mg, Si and F, phengites in the ore carry Cu (up to 1 wt.%); in colusite-bearing ore, trace quantities of Ge were detected (40 to 160 ppm, rarely 600 to 1100 ppm Ge).

Euhedral tourmaline 10 to 70 μm in size is frequently associated with muscovite (Fig. 5h). Rims are pure dravite (Mg-numbers close to 100, low in Ca and Ti,

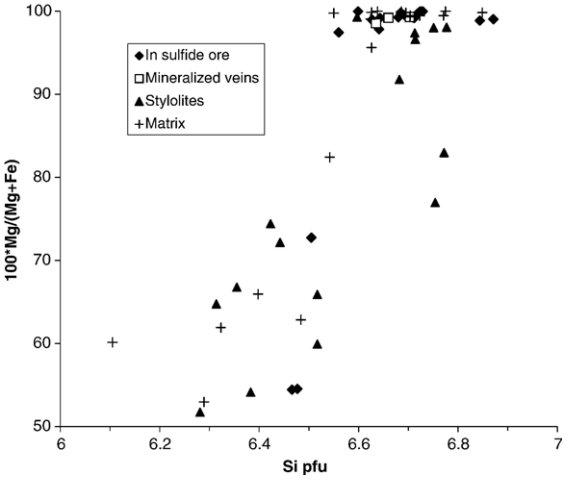

Fig. 9. Diagram of Si per formula unit (pfu) versus 100*Mg/(Mg+Fe) for white mica from the Khusib Springs deposit.

high in Na and F), whereas the cores have higher concentrations of Fe, Ti and Ca. Accessory potassium feldspar in mineralized samples is $Or_{>97}Ab_{<2}An_{<1}$. Fluor-apatite is moderately abundant in the mineralized section, and quartz is very rare in both ore and host rocks.

7. Discussion

7.1. Khusib Springs — a Tsumeb-type deposit?

The Tsumeb deposit is the type locality for polymetallic pipe-like deposits hosted by karst-controlled solution cavities in carbonate successions. It is distinguished from stratiform and strata-bound carbonate-hosted Pb–Zn deposits (e.g., the Mississippi Valley-type deposits, MVT) by high Cu and As as well as unusual trace element contents, and a very complex mineralogy (Table 7; Melcher, 2003). Estimated reserves of Ge in the Tsumeb pipe prior to mining were 2160 tons (Lombaard et al., 1986). Although only 87 tons of Ge were recovered between 1950 and 1968 (Schneider, 1992), Namibia was a major world supplier during this period. Germanium is irregularly distributed in the Tsumeb deposit. Average run-of-mill ore contained about 50 ppm Ge. Underground sections with up to 28 t of massive germanite have been mined in the upper levels and made Tsumeb unique (Lombaard et al., 1986). Recent analyses of sulfide-bearing drill core samples from the 30, 37 and 44 levels range from less than 5 up to 1000 ppm Ge, and Cu/Ge ratios vary by several orders of magnitude from 300 to 30,000. Assays of Ge-rich ore from Tsumeb collections yield more than 1% Ge, along with significant Ga (to 1%), Mo (to 1%), W (to 0.4%) and As (3 to 4%). The main hosts of Ge are germanite [$Cu_{26}Fe_4Ge_4S_{32}$], reniérite [$(Cu,Zn)_{22}(Ge,As)_4Fe_8S_{32}$] and briartite [$Cu_2(Fe,Zn)GeS_4$], which is restricted to massive germanite ore. Germanite and reniérite usually occur as small anhedral to subhedral crystals 10 to 100 μm size in association with tennantite, sphalerite, bornite, digenite, pyrite and galena. Germanite was present in the Tsumeb pipe from the surface down to 31 level, whereas reniérite is only known below level 15. Accordingly, germa-

Table 7
Comparison of some characteristics of Tsumeb, Khusib Springs and Berg–Aukas-type base metal sulfide deposits (sources: Chetty and Frimmel, 2000; Frimmel et al., 1996; Hughes, 1987; Lombaard et al., 1986; Pirajno and Joubert, 1993)

	Tsumeb	Khusib Springs	Berg Aukas-type
Host rock	Elandshoek and Hüttenberg Formations (dolomites) T4 through T8 zones	Maieberg Formation (laminated limestone), below T2/T3 contact	Abenab Subgroup and lower Tsumeb Subgroup
Shape of orebody	Discordant pipe, filled with breccia and sandstone; structural control	Stratiform lens, dolomite breccia; structural control	Stratiform lenses, discordant breccias
Ore mineralogy	Tn, Ga, Sph, Py, Bn, Cp, germanite, reniérite	Tn, En, Ga, Sph, Py (Cp, Bn), Ge–colusite, Ag–sulfosalts	Sph, Ga (Py, Cp, Tn)
Ore geochemistry	Pb>Cu=Zn. Considerable As, Ag, Cd, Ge, Ga, W	Cu>Pb>Zn. Considerable As, Sb, Ag, Ge, Cd, Hg	Zn>Pb; supergene V; low Cu, Ag, As, Ge, Ga, Cd
$\delta^{34}S$ [‰ CDT]	+13 to +24	+21 to +28	+17 to +30
Pb–isotopes	"Tsumeb trend"	"Khusib trend"	"Berg Aukas trend "
$\delta^{13}C$ [‰ SMOW] (carb.)	−4 to +2	−3 to +1	+3 to +5
Fluid inclusions	22 ± 3 wt.% NaCl eq. >212 °C (dolomite III)	20 ± 4 wt.% NaCl eq. >291 °C (dolomite III)	ca. 23 wt.% NaCl eq. 137 to 255 °C
Fluid source	Orogenic fluids	Orogenic fluids	Basinal brines
Age	460 to 530 Ma ?	Unknown	635 to 750 Ma ?
Oxidation	Locally strong	Weak	Variable

Abbreviations: Bn, bornite; Cp, chalcopyrite; En, enargite; Ga, galena; Py, pyrite; Sph, sphalerite; Tn, tennantite.

nite/reniérite ratios decrease with depth (Lombaard et al., 1986). Textural relations indicate that germanite replaces reniérite in most cases, although the opposite has been observed as well. A number of minerals carrying both Ge and V were reported from the Tsumeb mine by Geier and Ottemann (1970a,b), who identified Ge-bearing sulvanite [$Cu_3(Ge,V)S_4$] and V-bearing germanite. Sulvanite contains more V, and germanite has more Fe and Ge than colusite at Khusib (Fig. 8b). Tungsten-germanite carrying 7.4 to 10.3 wt.% W was also found in Tsumeb, and is reported to commonly develop crystal morphologies (Geier and Ottemann, 1970a), similar to the W- and Ge-bearing colusite described from Khusib Springs in the present study. Germanocolusite with a general formula of [$Cu_{26}V_2(Ge,As)_6S_{32}$] and $Ge/(Ge+As)>0.5$ was described from Tsumeb by Spiridonov et al. (1992). Spiridonov (1994, 2003) also identified Ge-, Mo- and W-rich sulfides associated with germanocolusite, namely maikainite [$Cu_{20}(Fe,Zn,Cu)_6Mo_2Ge_6S_{32}$] and ovamboite [$Cu_{20}(Fe,Zn,Cu)_6W_2Ge_6S_{32}$]. Reniérite, germanite, colusite (Fig. 8b) and sulvanite are structurally closely related minerals of the fahlore group (Bernstein, 1986; Spry et al., 1994).

Stannoidite, previously not known from the Tsumeb mine, is described here for the first time from Tsumeb (drill core from the 30 level) and Khusib Springs. Stannoidite carries up to 2.2 wt.% Ge at Tsumeb, and up to 0.7 wt.% Ge at Khusib.

The mineralization at Khusib Springs shares many features with the Tsumeb deposit. Accordingly, Chetty et al. (1997) and Chetty and Frimmel (2000) classify the deposit as a Tsumeb-type deposit, possibly representing the root zone of a much larger deposit higher up in the stratigraphic sequence and now eroded. Features similar between Tsumeb and Khusib Springs are: (1) the relation to syn-D_2 structures, i.e., folding; (2) the general chemistry of the ore — dominated by Cu; variable Pb, Zn; elevated concentrations of trace metals such as Ag, Ge, V, Sn, Mo, W; (3) the heavy sulfur isotope compositions; (4) the major hypogene mineral assemblage consisting of tennantite, galena, sphalerite, pyrite, with low contents of chalcopyrite, (5) the presence, in trace amounts, of minerals typical of the primary and secondary Tsumeb assemblage.

Major differences to Tsumeb are: (1) generally higher concentrations of Sb and Ag in fahlore and bulk ore; (2) the presence of large amounts of enargite, being the second most abundant Cu mineral in the deposit — at Tsumeb enargite was present only in the upper part of the mine (Lombaard et al., 1986); (3) the virtual absence of bornite; (4) the presence of Ag-sulfosalts unknown from Tsumeb; (5) the presence of Ge-bearing colusite as the major carrier of Ge instead of germanite and reniérite at Tsumeb; (6) the lack of pervasive oxidation below the surface; (7) dolomite prevails at Khusib, whereas calcite and quartz are the dominant alteration minerals, syngenetic with sulfides, at Tsumeb (Gross and Vollbrecht 2003; Melcher et al., 2003).

Compositional variations of the major sulfide minerals in the Khusib Springs and Tsumeb deposits are overall small (Table 6). Fahlore from Khusib carries more Sb, Ag, Mn and less Cd than fahlore from Tsumeb (own, unpublished data from sulfide ore at levels 30 and 37; Lombaard et al., 1986). Enargite is an important carrier of Ge (500 ppm reported for Tsumeb; Lombaard et al., 1986; 550 ppm as an average for sample KS-03 from Khusib). Galena is not a major carrier of Ag in both deposits, and pyrite is usually Cu-bearing but has low concentrations of Co, Ni and As. Sphalerite from Tsumeb is richer in Ga and Cd than sphalerite I and II from Khusib; however, variable Fe concentrations reported in the literature (Emslie and Beukes, 1981) suggest that more than one sphalerite generation is developed at Tsumeb.

In some carbonate-hosted Zn–Pb deposits of the MVT-type, and also in some sediment-hosted Zn–Pb deposits (e.g., Red Dog, Alaska; Kelley et al., 2004), up to 3000 ppm Ge are hosted by sphalerite and wurtzite. Average Ge concentrations in zinc concentrates of such deposits may reach a few hundred parts per million (Höll et al., this volume). Substitution of Ge for Zn in sphalerite is favored at low temperature and relatively low sulfur fugacity (Bernstein, 1985; Johan, 1988). Differences in sphalerite composition between MVT and Tsumeb-type deposits are attributed to thermal regimes and probably solution chemistries. MVT formed from saline low-temperature fluids (commonly 100 to 200 °C; e.g., Misra, 2000, for a summary), commonly during global-scale tectonic events (Leach et al., 2001), whereas Tsumeb-type mineralization formed from considerably hotter fluids, as discussed below.

The conditions under which base metal deposits in the OML formed are a matter of considerable debate. Agreement has been achieved that Berg Aukas-type deposits formed from basinal brines (~23 wt.% NaCl equivalent, <240 °C, $\delta^{18}O_{fluid}+13‰$) moving along aquifers in the basal Damara Supergroup during an extensional period, probably during diagenesis (Table 7; Pirajno and Joubert, 1993; Frimmel et al., 1996). Conditions inferred for Berg Aukas-type deposits thus resemble MVT deposits. In contrast, timing of ore

deposition, fluid temperature and salinity data are controversially discussed for Tsumeb-type deposits. While Hughes (1987) and Maiden and Hughes (2000) discuss a pre-D_2 mineralising event for Tsumeb, most authors agree that Tsumeb-type deposits formed during metamorphism and regional D_2 deformation (Lombaard et al., 1986) from hot fluids (350 to 450 °C, $\delta^{18}O_{fluid}$ +18‰; Frimmel et al., 1996) that moved along regional structures and precipitated ores in traps such as karst structures (Table 7). However, pre-D_2 ores were found locally (e.g., Fe–Mn ores and stratiform Cu ores at Kombat; Frimmel et al., 1996). Haynes (1984) interpreted the hypogene ore at Tsumeb to have resulted from interaction of Cu–As-rich, warm (210 to 280 °C), moderately saline (6 to 12 wt.% NaCl equiv.) circulating fluids with host dolomites. Lombaard et al. (1986) refer to homogenization temperatures for fluid inclusions in early quartz in the range of 230 to 250 °C and lower salinities (2 to 7 wt.% NaCl equiv.). Fluid salinity is reported to increase, while CO_2 contents decrease with depth in the Tsumeb pipe. A confining pressure of 500 to 700 bars was estimated, and the age of the mineralization was thought to be 580 to 530 Ma (syn-D_2) based on Pb–Pb isotope compositions of galena (Lombaard et al., 1986; Kamona et al., 1999). In contrast, Chetty and Frimmel (2000) obtained fluid inclusion homogenization temperatures up to 212 °C for dolomite III and 131 °C for calcite II at Tsumeb, and up to 291 °C for dolomite II at Khusib Springs. Their measured salinities are considerably higher than previous data, i.e., 22 ± 3 wt.% NaCl equiv. for Tsumeb and 20 ± 4 wt.% NaCl equiv. for Khusib Springs. If a syn-metamorphic, syn-deformational mineralization event is accepted for the Tsumeb and Khusib Springs deposits, a lithostatic pressure of 2.5 kbar and temperatures in excess of 300 °C are reasonable estimates for the time of mineralization (Frimmel et al., 1996). Pressure corrections to the fluid inclusion data yield formation temperatures of 275 °C for dolomite III at Tsumeb, and 370 °C for dolomite II at Khusib Springs (Chetty and Frimmel, 2000).

Stable isotope data ($\delta^{13}C$, $\delta^{18}O$) of ore-bearing dolomite II at Khusib Springs point to a metamorphic origin of the mineralizing fluids (Chetty and Frimmel, 2000). High concentrations of REE in carbonates suggest mineralizing fluids having interacted extensively with rocks underlying the Otavi Group. The highly saline fluids are dominated by Ca- and Mg-chloride with subordinate NaCl, indicative of a large component of evaporitic residual brines (Chetty and Frimmel, 2000).

Sulfur isotope ratios of sulfides in the OML are rather uniform, with only few exceptions. At Khusib Springs, $\delta^{34}S$ in all types of mineralization range from +20.8‰ to +27.8‰ (Table 2; Fig. 6). Sulfides from the Tsumeb deposit and from Berg Aukas-type Zn–Pb deposits range from +17.0‰ to +30‰ (own unpublished data; Hughes, 1987; Table 7). In contrast, a much wider spread is reported for sulfides of the Kombat mine (−11‰ to +26‰; Hughes, 1987; Pirajno and Joubert, 1993), which, according to current views, is also a member of the 'Tsumeb-type' (Hughes, 1987; Frimmel et al., 1996). The heavy sulfur isotopes of the Khusib Springs, Tsumeb and Berg Aukas sulfides are unique among carbonate-hosted base metal sulfide deposits, and most probably indicate derivation from sedimentary sulfate minerals, which precipitated from contemporaneous seawater. The narrow range of sulfide $\delta^{34}S$ suggests abiologic reduction processes (e.g., Misra, 2000). Evaporite horizons in the upper Nosib Group may be possible sources of the sulfate component. Hughes (1987) recognized an evaporite horizon carrying gypsum and anhydrite ($\delta^{34}S = 31‰$ to 33‰) in the upper Tsumeb Subgroup (T7 zone) of the Tsumeb area, which may have acted as a source for sulfur in the Tsumeb deposit.

Based mainly on Pb isotope work, Hughes (1987) favors pelitic rocks of the Kombat Formation (Fig. 1), metal-rich dolostone of the T8 zone and phosphoritic dolostone of the Hüttenberg Formation as sources of base metals and many other elements. Volcanic rocks and impure sandstones of the Nosib Group may also have contributed base metals to through-flowing brines which moved along different aquifer systems to deposit the metals. Chetty and Frimmel (2000) argue that the Grootfontein ultramafic–mafic body in the basement of the Otavi Mountain Land may have served as an additional source of base metals. Lead isotope ratios of the Khusib Springs sulfide ores suggest mixing of a hydrothermal source similar to the one envisaged for Tsumeb- and Berg Aukas-type deposits, with lead from a different source (Fig. 7). That source is probably not identical with clastically influenced, laminated limestones of the Maieberg Formation (T2 zone) in the footwall of the Khusib Springs orebody: the limestones host stratiform, subeconomic mineralization of pyrite and pyrrhotite with minor chalcopyrite and sphalerite, which are characterized by higher $^{206}Pb/^{204}Pb$ (unpublished data, Ongopolo), and rather light sulfur isotope ratios ($\delta^{34}S$, −24‰ to 0‰; unpublished data).

7.2. Formation of the Khusib Springs deposit

The lens-shaped orebody of Khusib Springs is developed along a breccia horizon attributed to hydrother-

mally induced solution-collapse preceding, or during regional D_2 deformation. The footwall mineralization with Fe-bearing sphalerite I, chalcopyrite, pyrite and minor Fe-rich tennantite is the earliest mineralization phase. In the massive Cu ore, chalcopyrite and bornite represent early mineralization, because they only occur as inclusions in early pyrite (Table 1), along with sphalerite II. The early-stage mineralization was essentially free of arsenic. It is replaced by main-stage enargite and tennantite, which display inconsistent relationships to each other. The general tendency, however, is that of tennantite replacing enargite. Ge-bearing colusite, pearceite–polybasite, galena and some pyrite are in equilibrium with enargite and tennantite, but not with sphalerite I or II. Occasionally, Ag-bearing enargite is rimmed by an Ag-rich fahlore-like phase towards surrounding tennantite. Enargite and tennantite are replaced by chalcocite-group minerals (digenite), constituting the main minerals of the late stage and finally, by covellite. Digenite is associated with late-stage sphalerite III (Cu, Ag-rich), tetrahedrite and pearceite–polybasite, which are associated with development of a considerable secondary porosity.

Thermodynamic calculations indicate that tennantite is a relatively low-temperature mineral in the system Cu–Fe–As–S–O–H (Schwartz, 1995). Chalcopyrite and bornite are stable at higher temperature and/or Cu^+/H^+ ratios, underlining the textural observation that both are relict minerals formed earlier at higher temperatures, and were later replaced by tennantite and enargite. Furthermore, co-precipitation of pyrite and tennantite is favored by relatively high H_3AsO_3 and H_2S activities, high oxygen fugacities and high temperatures (Schwartz, 1995). Möller (1985) proposed the use of Ga/Ge ratios in sphalerite to estimate the conditions of sphalerite deposition under the assumption that Ga/Ge ratios in the fluid equal those in sphalerite. Sphalerite II from the upper zone of the Khusib orebody (800 ppm Ga,<30 ppm Ge) has log (Ga/Ge)>1.4 corresponding to $T>260\pm10$ °C. In comparison, Ga-rich sphalerite from Tsumeb yields temperatures close to 300 °C. Temperature and sulfur fugacity are constrained by the occasional presence of stannoidite (Lee et al., 1975; Shimizu and Shikazono, 1987). The association of stannoidite with chalcopyrite would record lower sulfur fugacity than the association with bornite+pyrite. In the presence of Fe-poor sphalerite and tennantite, stannoidite stability ranges from 200 to 300 °C and $10^{-15}<\log fS_2<10^{-7}$ atm (Shimizu and Shikazono, 1987). High temperatures and sulfur fugacities are also in accordance with the presence of Ge-bearing colusite. Furthermore, the pentavalent state of As and the tetravalent state of Ge in the colusite structure (Frank-Kamenetskaya et al., 2002) indicate that colusite forms under relatively high fO_2 conditions, similar to Ge-bearing colusite associated with pyrite, chalcopyrite and bornite in volcanogenic sphalerite–barite ores at the Yanahara mine, Japan (Kase et al., 1994).

Main-stage sulfides are intergrown with iron-free, phengitic F-rich white mica and dravitic tourmaline, which differ chemically from sericitic mica and tourmaline in the dolomite host rock (Fig. 9). It is thus assumed that an Mg–F-rich hydrothermal fluid replaced detrital or diagenetic silicates, and precipitated hydrothermal silicates. Using the sericite boundary reactions formulated by Crerar and Barnes (1976) and assuming K^+ activity of 0.5, the fluid pH is fixed to values between 3 and 5 by the stability of muscovite, but may have changed to lower values due to the occasional presence of kaolinite (Fig. 5h). The zonation with tennantite+enargite in the central, and tennantite+sphalerite in the marginal parts of the Khusib Springs orebody would be best explained by pH increase due to interaction of an acid, hot, saline hydrothermal fluid with host carbonates. Constraints on the physico-chemical conditions of sulfide precipitation at Khusib are in close agreement with estimates for the Tsumeb deposit. Hughes (1987) gave values of $10^{-39}<\log fO_2<10^{-33}$ atm, $\log fS_2>10^{-8.5}$, and fluid pH of 3 to 6.

7.3. Enrichment of Ge at Khusib Springs

Germanium and silicon are geochemically closely related and thus, Ge/Si ratios are fairly similar (10^{-6}) in the crust and in rivers, unless there is organic matter involved. However, significant fractionation may occur in hydrothermal fluids (Ge/Si=10^{-5} to 10^{-3}; Pokrovski and Schott, 1998). Germanium is transported in dilute aqueous hydrothermal fluids as neutral hydroxide species $[Ge^{4+}(OH)_4^0(aq)]$ at pH values<8 over a wide range of temperatures (20 to 350 °C). The negatively charged hydroxide complexes $[GeO(OH)_3^-(aq)]$ develop only at pH>8 (Pokrovski and Schott, 1998). These authors showed that the solubility of Ge and Ge/Si ratios in thermal waters increase with temperature and salinity. Germanium is also enriched in high-temperature hydrothermal systems associated with granitoids, e.g., in topaz, fluorite, and white mica (Bernstein, 1985), suggesting Ge-transport as H_2GeF_6 complexes. However, experimental data show that significant Ge-fluoride complexes may form occur only in very acid (pH<3) F-rich solutions (Ciavatta et al.,

1990). Sulfur-bearing Ge species possibly also form in S-rich hydrothermal fluids (Bernstein, 1985).

Concentration through magmatic fractional crystallisation, or uptake from country rocks by fluids may be considered viable sources of Ge in a deposit. The latter is favored for Khusib Springs, because there are no time-equivalent magmatic rocks in the OML. Favorable country rocks from which Ge may be mobilized are sediments containing organic material, such as the Maieberg limestones (T2-zone) in the footwall of the deposit. Organic matter of unknown origin has accumulated along stylolites, and is present in disseminated form throughout the succession. Lignin-derivative organic compounds as found in peat and lignite account for the concentration of Ge in coals and related organic material (Bernstein, 1985). The strong biophile affinity of Ge makes some large coal deposits potential targets for future Ge production (Höll et al., this volume).

At Khusib Springs, textural and geochemical evidence indicates a close link between Cu-sulfosalts (enargite, tennantite) and Cu-thiogermanate minerals (Ge-bearing colusite, germanite) with F-rich phengitic mica (carrying traces of Ge), F-rich dravitic tourmaline, kaolinite, rutile and (semi)graphite; quartz is notably lacking. The element association of Ge with V, Sn, Mo and W points to the involvement of an organic compound. It has been demonstrated above that the sulfide ores precipitated at elevated oxygen fugacities from hot (>300 °C), saline, metal-rich fluids. Fluid inclusion data, analyses of fluid inclusion leachates (Chetty and Frimmel, 2000), and sulfur isotope compositions indicate an evaporitic component to the fluids. This would also explain the concentration of fluorine in hydrothermally formed mica and tourmaline. The close association of F-rich silicates with Ge-bearing sulfides may point to the presence of Ge-fluoride complexes in the fluid; the necessary low pH values are corroborated by the presence of kaolinite. Destabilisation of Ge complexes in the fluid may be caused by a drastic pH increase along sulfide–dolomite contacts, where most of the colusite is located.

The polyphase mineral assemblage (Table 1) and geochemical zoning of the orebody (Figs. 3, 6, Table 5) imply a complex model of ore formation. The early stage-mineralization of sphalerite, pyrite and minor galena and Fe-rich tennantite formed from a hot, saline hydrothermal fluid at relatively lower fS_2 and fO_2 than the main stage Ge-rich mineralization dominated by tennantite and enargite. Early stage mineralization shares some aspects of mineralization commonly referred to as Berg Aukas-type in the OML, and with MVT deposits; this point needs further clarification. Ample textural evidence of replacement of early stage ore by main stage ore indicates that an upgrading or enrichment process took place. The late stage mineralization with Ag- and Cu-rich Zn sulfide, digenite, pearceite–polybasite and tetrahedrite clearly postdates this replacement process, and must be attributed to fluid-induced remobilisation of parts of the orebody at lower temperatures.

8. Implications for exploration on Ge-rich ores in the OML

The present study of the Khusib Springs deposit in the Otavi Mountain Land reveals several points relevant for exploration strategies for similar trace element-rich base metal orebodies. Khusib Springs could not be located using the geophysical and geochemical exploration methods available to the mining companies. Despite the stratigraphic position of Tsumeb in the upper part of the Tsumeb Subgroup (T4 through T8 zones), the location of Khusib Springs within the lowermost section of the Subgroup (T2/T3 contact) highlights its potential to host "Tsumeb-type" Ge-rich sulfide mineralization. Enrichment of Ge in the Khusib Springs, and probably Tsumeb, deposits is a result of a number of factors, including (1) high fluid temperature, (2) high salinity, (3) high concentrations of S, As, Mg, F in the fluid, (4) the presence of sediments rich in degraded organic material (e.g., the Maieberg limestones, T2) where organophile trace elements may have accumulated (Ge, V, Sn, Mo, W), (5) the presence of structures focussing fluid flow (pre-D_2 and syn-D_2 fractures, faults and shear zones), and (6) the presence of traps, such as breccia bodies or karst pipes. The presence of sandstone-filled karst pipes is not a prerequisite to Ge mineralization; however, it may well be responsible for the relative enrichment of Ga in Tsumeb ores compared to Khusib Springs.

Therefore, known mineral occurrences, for example in the Maieberg Formation, are worth-wile exploration targets. The contact between the Abenab Subgroup (Auros Formation) and the Maieberg Formation of the lower Tsumeb Subgroup is known to host "Berg Aukas-type" Zn–Pb(–V) mineralization in the Abenab area to the northeast of Khusib Springs. Furthermore, a number of mineral occurrences in the Harasib–Olifantsfontein syncline have been attributed to Berg Aukas-type mineralization. Upgrading of such Zn-rich deposits by later fluids percolating along favorable structures may have produced similar orebodies as at Khusib. The highly mineralized area of the Otavi Valley in the southern Otavi Mountain Land hosts 'Tsumeb-type deposits' also in strata of the lower Tsumeb Subgroup.

Preliminary data show that some of these deposits have above-background concentrations of Ge. Therefore, the complete Tsumeb Subgroup has a high potential for undiscovered, exceptionally rich polymetallic sulfide orebodies.

Acknowledgements

The support by Ongopolo Mining Ltd., especially by its manager, A. Neethling, and by geologists A. Günzel and A. Lombaard, is much appreciated. We gratefully acknowledge assistance by Dr. G. Schneider and V. Petzel from the Geological Survey of Namibia. H. Frimmel (University of Cape Town, now University of Würzburg) kindly provided unpublished material. Geochemical analyses were ably carried out by J. Lodziak (EMP) and F. Korte (XRF). SIMS analyses were performed by S. Chryssoulis (AMTEL, Canada). Discussions with C. Gross, A. Vollbrecht (University of Göttingen), M. Brauns, J. Schneider and U. Haack (University of Giessen) are also acknowledged. Critical reviews by H. Frimmel and an anonymous referee improved the paper. Valuable comments and suggestions by U. Schwarz–Schampera are much appreciated.

References

Allsopp, H.L., Welke, H.J., Hughes, M.J., 1981. Shortening the odds in exploration. Nuclear Active 24, 8–12.

Barkov, A.Y., Martin, R.F., Poirier, G., Men'shikov, Y.P., 2000. Zoned tungstenoan molybenite from a fenitized megaxenolith in the Khibina alkaline complex, Kola Peninsula, Russia. Canadian Mineralogist 38, 1377–1385.

Bernstein, L.R., 1985. Germanium geochemistry and mineralogy. Geochimica et Cosmochimica Acta 49, 2409–2422.

Bernstein, L.R., 1986. Renierite, $Cu_{10}ZnGe_2Fe_4S_{16}$–$Cu_{11}GeAsFe_4S_{16}$: a coupled solid solution series. American Mineralogist 71, 210–221.

Cairncross, B., 1997. The Otavi Mountain Land Cu–Pb–Zn–V deposits, Namibia. Mineralogical Record 28, 109–157.

Chetty, D., Frimmel, H.E., 2000. The role of evaporites in the genesis of base metal sulfide mineralization in the Northern Platform of the Pan-African Damara Belt, Namibia: geochemical and fluid inclusion evidence from carbonate wall rock alteration. Mineralium Deposita 35, 364–376.

Chetty, D., Verran, D., Frimmel, H.E., le Roex, A.P., 1997. The Khusib Springs Cu–Pb–Zn–Ag Deposit, Otavi Mountain Land, Namibia. Mineralization of the "Tsumeb-type"? In: Papunen, H. (Ed.), Mineral Deposits: Research and Exploration — Where Do they Meet? Balkema, Rotterdam, pp. 531–534.

Chryssoulis, S.L., Cabri, L.J., Lennard, W., 1989. Calibration of the ion microprobe for quantitative trace precious metal analyses of ore minerals. Economic Geology 84, 1684–1689.

Ciavatta, L., Iuliano, M., Porto, R., Vasca, E., 1990. Fluorogermanate(IV) stabilities in acid media. Polyhedron 9, 1263–1270.

Coakley, G.J., 1997. The mineral industry of Namibia. USGS Minerals Yearbook, Area reports, International, vol. III, pp. DD1–DD7.

Coakley, G.J., 2000. The mineral industry of Namibia. USGS Minerals Yearbook, Area reports, vol. III, pp. 23.1–23.6.

Crerar, D.A., Barnes, H.L., 1976. Ore solution chemistry V. Solubilities of chalcopyrite and chalcocite assemblages in hydrothermal solution at 200° to 350 °C. Economic Geology 71, 772–794.

Ebel, D.S., Sack, R.O., 1991. Arsenic–silver incompatibility in fahlore. Mineralogical Magazine 55, 521–528.

Emslie, D.P., Beukes, G.J., 1981. Minor- and trace-element distribution in sphalerite and galena from the Otavi Mountainland, South West Africa. Annals of the Geological Survey, Republic of South Africa 15/2, 11–28.

Fölling, P.G., Frimmel, H.E., 2002. Chemostratigraphic correlation of carbonate successions in the Gariep and Saldania Belts, Namibia and South Africa. Basin Research 14, 69–102.

Frank-Kamenetskaya, O.V., Rozhdestvenskaya, I.V., Yanulova, L.A., 2002. New data on the crystal structures of colusites and arsenosulvanites. Journal of Structural Chemistry 43, 89–100.

Frimmel, H.E., Frank, W., 1998. Neoproterozoic tectono-thermal evolution of the Gariep belt and its basement, Namibia/South Africa. Precambrian Research 90, 1–28.

Frimmel, H.E., Deane, J.G., Chadwick, P.J., 1996. Pan-African tectonism and the genesis of base metal sulfide deposits in the northern foreland of the Damara orogen, Namibia. Society of Economic Geologists Special Publication 4, 204–217.

Geier, B.H., Ottemann, J., 1970a. New secondary tin–germanium and primary tungsten–(molybdenum–vanadium) germanium minerals from the Tsumeb ore deposit. Neues Jahrbuch für Mineralogie Abhandlungen 114, 89–107.

Geier, B.H., Ottemann, J., 1970b. New primary vanadium-, germanium-, gallium-, and tin-minerals from the Pb–Zn–Cu deposit Tsumeb, South West Africa. Mineralium Deposita 5, 29–40.

George, M.W., 2003. Germanium. USGS, Minerals Yearbook, pp. 31.1–31.5.

George, M.W., 2005. Germanium. USGS, Mineral Commodity Summaries, January 2005, pp. 70–71.

Gross, C., Vollbrecht, A., 2003. Cathodoluminescence studies on carbonates from the Otavi Mountain Land, Namibia. Interim Report "BGR-Hochschulvergabeprojekt 81". GWZ Universität Göttingen. 49 pp.

Haynes, F.M., 1984. A geochemical model for sulfide paragenesis and zoning in Cu–Fe–As–S systems (Tsumeb, South West Africa/Namibia). Chemical Geology 47, 183–190.

Hedberg, R.M., 1979. Stratigraphy of the Ovamboland Basin, South West Africa. Chamber of Mines Precambrian Research Unit, University of Cape Town 24. 325 pp.

Hoffman, P.F., Kaufman, A.J., Halverson, G.P., Schrag, D.P., 1998. A neoproterozoic snowball Earth. Science 281, 1342–1346.

Hoffman, K.H., Condon, D.J., Bowring, S.A., Crowley, J.L., 2004. U–Pb zircon date from the neoproterozoic ghaub formation, Namibia: constraints on Marinoan glaciation. Geology 32, 817–820.

Höll, R., Weber-Diefenbach, K., 1973. Tungstenit–Molybdänit–Mischphasen in der Scheelitlagerstätte Felbertal (Hohe Tauern, Österreich). Neues Jahrbuch für Mineralogie, 27–34.

Höll, R., Kling, M., Schroll, E., this volume. Germanium: geochemistry, mineralogy, geology, and economics — a review. Ore Geology Reviews.

Hughes, M.J., 1987. The Tsumeb orebody, Namibia, and related dolostone-hosted base metal deposits of Central Africa. Ph.D. thesis, University of the Witwatersrand, Johannesburg, South Africa. University Microfilms International, Ann Arbor, Michigan. 448 pp.

Johan, Z., 1988. Indium and germanium in the structure of sphalerite: an example of coupled substitution with copper. Mineralogy and Petrology 39, 211–229.

Kamona, A.F., Léveque, J., Friedrich, G., Haack, U., 1999. Lead isotopes of the carbonate-hosted Kabwe, Tsumeb, and Kipushi Pb–Zn–Cu sulfide deposits in relation to Pan African orogenesis in the Damaran–Lufilian fold belt of Central Africa. Mineralium Deposita 34, 273–283.

Kase, K., Yamamoto, M., Mitsuno, C., 1994. Germanium-bearing colusite from the Yanahara mine, Japan, and its significance to ore genesis. Resource Geology 44, 33–38.

Kaufman, A.J., Hayes, J.M., Knoll, A.H., Germ, G.J.B., 1991. Isotopic composition of carbonates and organic carbon from upper Proterozoic successions in Namibia: stratigraphic variation and the effects of diagenesis and metamorphism. Precambrian Research 49, 301–327.

Kelley, K.D., Leach, D.L., Johnson, C.A., Clark, J.L., Fayek, M., Slack, J.F., Anderson, V.M., Ayuso, R.A., Ridley, W.I., 2004. Textural, compositional, and sulfur isotope variations of sulphide minerals ion the Red Dog Zn–Pb–Ag deposits, Brooks Range, Alaska: implications for ore formation. Economic Geology 99, 1509–1532.

Kennedy, M.J., Runnegar, B., Prave, A.R., Hoffmann, K.-H., Arthur, M.A., 1998. Two or four Neoproterozoic glaciations? Geology 26, 1059–1063.

Leach, D.L., Bradley, D., Lewchuk, M.T., Symons, D.T.A., de Marsily, G., Brannon, J., 2001. Mississippi Valley-type lead–zinc deposits through geological time: implications from recent age-dating research. Mineralium Deposita 36, 711–740.

Lee, M.S., Takenouchi, S., Imai, H., 1975. Syntheses of stannoidite and mawsonite and their genesis in ore deposits. Economic Geology 70, 834–843.

Lombaard, A.F., Günzel, A., Innes, J., Krüger, T.L., 1986. The Tsumeb lead–copper–zinc–silver deposit, South West Africa/Namibia. In: Anhaeusser, C.R., Maske, S. (Eds.), Mineral Deposits of Southern Africa, vol. II. Geological Society of South Africa, Johannesburg, pp. 1761–1787.

Maiden, K., Hughes, M.J., 2000. Mount Isa and Tsumeb: a comparative metallogenic study. Communications, Geological Survey of Namibia 12, 167–177.

Melcher, F., 2003. The Otavi Mountain Land in Namibia: Tsumeb, Germanium and Snowball Earth. Mitteilungen der Österreichen Mineralogischen Gesellschaft 148, 413–435.

Melcher, F., Oberthür, T., Vetter, U., Gross, C., Vollbrecht, A., Brauns, M., Haack, U., 2003. Germanium in carbonate-hosted Cu–Pb–Zn mineralization in the Otavi Mountain Land, Namibia. In: Eliopoulos, D. (Ed.), Mineral Exploration and Sustainable Development. Millpress, Rotterdam, pp. 701–704.

Misra, K.C., 2000. Understanding Mineral Deposits. Kluwer Academic Publishers, Dordrecht-Boston-London. 845 pp.

Möller, P., 1985. Development and application of the Ga/Ge-geothermometer for sphalerite from sediment-hosted deposits. Monograph Series on Mineral Deposits, vol. 25. Borntraeger, Berlin, pp. 15–30.

Oberthür, T., Rammlmair, D., Kojonen, K., 2000. Comparison of automated particle search techniques for platinum group elements (PGE) and minerals (PGM): μ-XRF and electron-microprobe. In: Rammlmair, D., et al., (Eds.), Applied Mineralogy. A.A. Balkema, Rotterdam, pp. 375–377.

Pirajno, F., Joubert, B.D., 1993. An overview of carbonate-hosted mineral deposits in the Otavi Mountain Land, Namibia: implications for ore genesis. Journal of African Earth Sciences 16, 265–272.

Pokrovski, G.S., Schott, J., 1998. Thermodynamic properties of aqueous Ge(IV) hydroxide complexes from 25 to 350 °C; implications for the behaviour of germanium and the Ge/Si ratio in hydrothermal fluids. Geochimica et Cosmochimica Acta 62, 1631–1642.

Schneider, G.I.C., 1992. Germanium and gallium. In: Hoal, B.G. (Ed.), The Mineral Resources of Namibia, Geological Survey of Namibia, pp. 3.4-1–3.4-2.

Schwartz, M.O., 1995. Arsenic in porphyry copper deposits: economic geology of a polluting element. International Geology Review 37, 9–25.

Shimizu, M., Shikazono, N., 1987. Stannoidite-bearing tin ore: mineralogy, texture and physicochemical environment of formation. Canadian Mineralogist 25, 229–236.

Spiridonov, E.M., 1994. New germanium–molybdenum–tungsten sulfide mineral phases from the massive sulfide–polymetallic Tsumeb deposit (Namibia). Geology of Ore Deposits 36, 335–341.

Spiridonov, E.M., 2003. Maikainite $Cu_{20}(Fe,Cu)_6Mo_2Ge_6S_{32}$ and ovamboite $Cu_{20}(Fe,Cu,Zn)_6W_2Ge_6S_{32}$: new minerals in massive sulphide base metal ores. Doklday Earth Sciences 393A, 1329–1332.

Spiridonov, E.M., Kachalovskaya, V.M., Kovachev, V.V., Krapiva, L.Ya., 1992. Germanocolusite $Cu_{26}V_2(Ge,As)_6S_{32}$: a new mineral. Vestnik Moskovskogo Universiteta, Seriya 4, Geologiya, 6, pp. 50–54 (in Russian).

Spry, P.G., Merlino, S., Wang, S., Zhang, X., Buseck, P.R., 1994. New occurrences and refined crystal chemistry of colusite, with comparison to arsenosulvanite. American Mineralogist 79, 750–762.

Verran, D., 1996. Genesis of the Khusib Springs Cu–Pb–Zn–(Ag) deposit, Otavi Mountain Land, Namibia. Hons Thesis, Department of Geological Sciences, University of Cape Town, Cape Town, South Africa, 30 pp.